



<sup>9</sup>Research Centre for Astronomy and Earth Sciences, Geodetic and Geophysical Institute, Sopron, Hungary

<sup>10</sup>School of GeoSciences, The University of Edinburgh, Edinburgh, UK

<sup>11</sup>Dept. of Earth Sciences, Royal Holloway, University of London (RHUL), Egham, UK

<sup>12</sup>Swiss Federal Laboratories for Materials Science and Technology (Empa), Dübendorf, Switzerland

<sup>13</sup>Atmospheric Chemistry Research Group, University of Bristol, Bristol, UK

<sup>14</sup>Italian National Agency for New Technologies, Energy and Sustainable Development (ENEA), Rome, Italy

<sup>15</sup>NOAA Earth System Research Laboratory, Global Monitoring Division, Boulder, CO, USA

<sup>a</sup>now at: Agenzia Regionale per la Protezione dell'Ambiente Ligure, Genova, Italy

<sup>b</sup>now at: Norwegian Institute for Air Research, Kjeller, Norway

<sup>c</sup>now at: Netherlands Organisation for Applied Scientific Research (TNO), Utrecht, the Netherlands

<sup>d</sup>now at: Institut für Umweltphysik, Heidelberg, Germany

<sup>e</sup>now at: Institute for Marine and Atmospheric research Utrecht, Utrecht University, Utrecht, the Netherlands

Received: 11 March 2014 – Accepted: 10 May 2014 – Published: 16 June 2014

Correspondence to: P. Bergamaschi (peter.bergamaschi@jrc.ec.europa.eu)

Published by Copernicus Publications on behalf of the European Geosciences Union.

## Top-down estimates of European CH<sub>4</sub> and N<sub>2</sub>O emissions

P. Bergamaschi et al.

Title Page

Abstract

Introduction

Conclusions

References

Tables

Figures



Back

Close

Full Screen / Esc

Printer-friendly Version

Interactive Discussion



## Abstract

European CH<sub>4</sub> and N<sub>2</sub>O emissions are estimated for 2006 and 2007 using four independent inverse modelling systems, based on different global and regional Eulerian and Lagrangian transport models. This ensemble approach is designed to provide more realistic estimates of the overall uncertainties in the derived emissions, which is particularly important for verifying bottom-up emission inventories.

We use continuous observations from 10 European stations (including five tall towers) for CH<sub>4</sub> and 9 continuous stations for N<sub>2</sub>O, complemented by additional European and global flask sampling sites. The available observations mainly constrain CH<sub>4</sub> and N<sub>2</sub>O emissions from north-western and eastern Europe. The inversions are strongly driven by the observations and the derived total emissions of larger countries show little dependence on the emission inventories used a priori.

Three inverse models yield 26–56 % higher total CH<sub>4</sub> emissions from north-western and eastern Europe compared to bottom-up emissions reported to the UNFCCC, while one model is close to the UNFCCC values. In contrast, the inverse modelling estimates of European N<sub>2</sub>O emissions are in general close to the UNFCCC values, with the overall range from all models being much smaller than the UNFCCC uncertainty range for most countries. Our analysis suggests that the reported uncertainties for CH<sub>4</sub> emissions might be underestimated, while those for N<sub>2</sub>O emissions are likely overestimated.

## 1 Introduction

Atmospheric methane (CH<sub>4</sub>) and nitrous oxide (N<sub>2</sub>O) are the second and third most important long-lived anthropogenic greenhouse gases (GHGs) after carbon dioxide (CO<sub>2</sub>). CH<sub>4</sub> and N<sub>2</sub>O have large global warming potentials of 28 and 265, respectively, relative to CO<sub>2</sub> over a 100 year time horizon (Myhre et al., 2013). Globally averaged dry-air mole fractions of CH<sub>4</sub> reached 1819 ± 1 ppb in 2012, 160 % above the

ACPD

14, 15683–15734, 2014

## Top-down estimates of European CH<sub>4</sub> and N<sub>2</sub>O emissions

P. Bergamaschi et al.

Title Page

Abstract

Introduction

Conclusions

References

Tables

Figures



Back

Close

Full Screen / Esc

Printer-friendly Version

Interactive Discussion



**Top-down estimates  
of European CH<sub>4</sub> and  
N<sub>2</sub>O emissions**

P. Bergamaschi et al.

Title Page

Abstract

Introduction

Conclusions

References

Tables

Figures



Back

Close

Full Screen / Esc

Printer-friendly Version

Interactive Discussion



pre-industrial level (1750) of  $\sim 700$  ppb, while N<sub>2</sub>O reached  $325.1 \pm 0.1$  ppb,  $\sim 20\%$  higher than pre-industrial level (270 ppb) (WMO, 2013). CH<sub>4</sub> and N<sub>2</sub>O contributed  $\sim 18\%$  and  $\sim 6\%$ , respectively, to the direct anthropogenic radiative forcing of all long-lived GHGs in 2012, relative to 1750 (NOAA Annual Greenhouse Gas Index (AGGI), <http://www.esrl.noaa.gov/gmd/aggi/>). CH<sub>4</sub> also has significant additional indirect radiative effects due to its feedback on global OH concentrations, tropospheric ozone, and stratospheric water vapour, and the generation of CO<sub>2</sub> as the final product of the CH<sub>4</sub> oxidation chain (Forster et al., 2007; Shindell et al., 2005). These indirect effects are reflected in the CH<sub>4</sub> emission-based radiative forcing of  $0.97$  ( $0.74$  to  $1.20$ ) Wm<sup>-2</sup>, which is about twice the concentration-based radiative forcing of  $0.48$  ( $0.43$  to  $0.53$ ) Wm<sup>-2</sup> (Myhre et al., 2013). In addition to its significant contribution to global warming, N<sub>2</sub>O plays an important role in the depletion of stratospheric ozone, with its current ozone depletion potential-weighted emissions being the largest of all ozone-depleting substances (Ravishankara et al., 2009).

On the European scale, combined emissions of CH<sub>4</sub> and N<sub>2</sub>O contributed  $15.2\%$  to total GHG emissions (in CO<sub>2</sub>-equivalents) reported under the United Nations Framework Convention on Climate Change (UNFCCC) by the EU-15 countries for 2011 ( $15.9\%$  for EU-27) (EEA, 2013). The large reductions of both CH<sub>4</sub> and N<sub>2</sub>O emissions (each by  $34\%$ ) since 1990 reported by the EU-15 contributed significantly to the reduction of its total GHG emissions by  $14.7\%$  (2011 compared to 1990), and will probably allow the EU-15 to over-achieve its collective target agreed under the Kyoto Protocol to reduce its average GHG emissions 2008–2012 by  $8\%$  compared to the base year 1990 (there is no common target for the EU-27 under the Kyoto Protocol) (EEA, 2013).

GHG emissions reported to the UNFCCC are based on statistical activity data and source-specific and country-specific emission factors (IPCC, 2006). For CH<sub>4</sub> and N<sub>2</sub>O however, such “bottom-up” emission inventories have considerable uncertainties, mainly due to the large variability of emission factors, which for many CH<sub>4</sub> and N<sub>2</sub>O sources are not very well characterized (e.g. CH<sub>4</sub> emissions from landfills, gas

production facilities and distribution networks, or N<sub>2</sub>O emissions from agricultural soils (e.g. Karion et al., 2013; Leip et al., 2011).

Complementary to “bottom-up” approaches, emissions can be estimated using atmospheric measurements and inverse modelling. This “top-down” technique is widely used to estimate GHG emissions on the global and continental scale (e.g. Bergamaschi et al., 2013; Bousquet et al., 2006; Hein et al., 1997; Houweling et al., 1999; Kirschke et al., 2013; Mikaloff Fletcher et al., 2004a, b for CH<sub>4</sub> and Hirsch et al., 2006; Huang et al., 2008; Thompson et al., 2014 for N<sub>2</sub>O). With the availability of quasi-continuous GHG measurements and increasing number of regional monitoring stations, especially in Europe and North America, various inverse modelling studies have estimated emissions also on the regional to country scale (e.g. Bergamaschi et al., 2010; Corazza et al., 2011; Kort et al., 2008; Manning et al., 2011), demonstrating the potential of using such top-down methods for independent verification of bottom-up inventories (Bergamaschi, 2007). The use of atmospheric measurements and inverse modelling for verification has also been recognized by the IPCC (IPCC, 2006).

Currently, only anthropogenic GHG emissions are reported to UNFCCC. In many specific cases, as the European CH<sub>4</sub> and N<sub>2</sub>O emissions discussed in this study, the contribution of natural emissions is considered to be relatively small. Nevertheless, quantitative comparison between inverse modelling and bottom-up estimates also requires estimates of natural emissions.

A further challenge with inverse modelling, particularly for its use in verifying bottom-up estimates, is the provision of realistic uncertainties for the derived emissions. Although various studies attempt to take into account estimates of the model representation and transport errors, such estimates are typically based on strongly simplified assumptions. As a complementary approach, the range of results from an ensemble of models can be analysed and may be considered as a more realistic estimate of the overall uncertainty, provided the applied models are largely independent and represent well the range of current models. Furthermore, detailed model comparisons, and verification with independent validation data, allow the model characteristics to be

## Top-down estimates of European CH<sub>4</sub> and N<sub>2</sub>O emissions

P. Bergamaschi et al.

[Title Page](#)[Abstract](#)[Introduction](#)[Conclusions](#)[References](#)[Tables](#)[Figures](#)[Back](#)[Close](#)[Full Screen / Esc](#)[Printer-friendly Version](#)[Interactive Discussion](#)

analysed in detail and potential model deficiencies to be identified. Comparisons of global inverse models have been performed for CO<sub>2</sub> (e.g. Peylin et al., 2013; Stephens et al., 2007), CH<sub>4</sub> (Kirschke et al., 2013) and N<sub>2</sub>O (Thompson et al., 2014), focussing on the global and continental scale. Here, we present for the first time a detailed comparison of inverse models estimating European CH<sub>4</sub> and N<sub>2</sub>O emissions. We use four inverse models, based on different global and regional Eulerian and Lagrangian transport models. The inversions are constrained by a comprehensive data set of quasi-continuous observations from European monitoring stations (including five tall towers), complemented by further European and global discrete air sampling sites.

## 2 Atmospheric measurements

The European monitoring stations used in the CH<sub>4</sub> and N<sub>2</sub>O inversions are summarized in Table 1. The monitoring stations include 10 sites with quasi-continuous measurements for CH<sub>4</sub> (i.e., providing data with hourly or higher time resolution), and 9 sites with quasi-continuous N<sub>2</sub>O measurements. Five of these stations are equipped with tall towers (Cabauw, Bialystok, Ochsenkopf, Hegyhatsal, and Angus), with uppermost sampling heights above the surface by 97–300 m. The measurements at the tall towers were set up or improved within the EU project CHIOTTO (“Continuous High-precisiOn Tall Tower Observations”) (Popa et al., 2010; Thompson et al., 2009; Vermeulen et al., 2011, 2007). Additional quasi-continuous measurements are from the AGAGE (Advanced Global Atmospheric Gases Experiment) network (Cunnold et al., 2002; Rigby et al., 2008) at Mace Head, from the operational network of the German Federal Environment Agency (UBA) at Schauinsland, from the Finnish Meteorological Institute at Pallas (Aalto et al., 2007), from the Swiss Federal Laboratories for Materials Science and Technology (EMPA) at Jungfrauoch, and from the Royal Holloway University of London (RHUL) in London. Furthermore, we use CH<sub>4</sub> and N<sub>2</sub>O discrete air samples from the NOAA Earth System Research Laboratory (ESRL) global cooperative air sampling network at 10 European sites (and for the global inverse models,

### Top-down estimates of European CH<sub>4</sub> and N<sub>2</sub>O emissions

P. Bergamaschi et al.

Title Page

Abstract

Introduction

Conclusions

References

Tables

Figures



Back

Close

Full Screen / Esc

Printer-friendly Version

Interactive Discussion



**Top-down estimates  
of European CH<sub>4</sub> and  
N<sub>2</sub>O emissions**

P. Bergamaschi et al.

Title Page

Abstract

Introduction

Conclusions

References

Tables

Figures



Back

Close

Full Screen / Esc

Printer-friendly Version

Interactive Discussion



additional global NOAA sites) (Dlugokencky et al., 1994, 2003, 2009), and CH<sub>4</sub> discrete air samples from the French RAMCES (Réseau Atmosphérique de Mesure des Composés à Effet de Serre) network (Schmidt et al., 2006) at 5 European sites. Finally, discrete air samples from the Max-Planck-Institute for Biogeochemistry at the Shetland Islands, and from the Italian National Agency for New Technologies, Energy and Sustainable Development (ENEA) at Lampedusa were used. Both quasi-continuous and discrete air sample measurements are based on Gas Chromatography (GC) using Flame Ionization Detectors (FID) for CH<sub>4</sub>, and Electron Capture Detectors (ECD) for N<sub>2</sub>O. Measurements are reported as dry air mole fractions (nmol mol<sup>-1</sup>, abbreviated as ppb).

For CH<sub>4</sub>, we generally apply the NOAA04 CH<sub>4</sub> standard scale (Dlugokencky et al., 2005) (AGAGE CH<sub>4</sub> data were converted to NOAA04 using a scaling factor of 1.0003 (Prinn et al., 2000), and RAMCES CH<sub>4</sub> data were scaled by 1.0124 from CMDL83 to NOAA04, (Dlugokencky et al., 2005). CH<sub>4</sub> comparisons of high pressure cylinders performed in the frame of the European projects MethMoniteur, IMECC, Geomon, and CHIOTTO and WMO between 2004 and 2010 showed that the CH<sub>4</sub> measurements of the CHIOTTO, NOAA, RAMCES, UBA, and RHUL networks agreed within 2 ppb. Furthermore, comparison of the quasi-continuous measurements at Pallas, Mace Head, Ochsenkopf, and Hegyhatsal with NOAA discrete air samples (using measurements coinciding within 1 h, and the additional condition that the quasi-continuous measurements show low variability within a 5 h time window) showed annual average absolute CH<sub>4</sub> biases of less than 4 ppb during 2006 and 2007, the target period of this study.

While the merged CH<sub>4</sub> dataset used in this study can, therefore, be considered as reasonably consistent, this is not the case for N<sub>2</sub>O, for which significant offsets are apparent between different monitoring laboratories, even though most laboratories use N<sub>2</sub>O primary standards from NOAA/ESRL. These offsets exceed the compatibility goal of  $\pm 0.1$  ppb ( $1\sigma$ ) recommended by WMO GAW (WMO, 2012) (Table 7). We, therefore, adopt the approach developed by Corazza et al. (2011) to correct for these calibration offsets in the inversion (see also Sect. 3), using the NOAA discrete air samples (which

are reported on the NOAA-2006 scale (Hall et al., 2007) as a common reference. Corazza et al. (2011) showed that the N<sub>2</sub>O bias correction derived in the inversion agreed within 0.1–0.2 ppb (N<sub>2</sub>O dry-air mole fraction) with the bias derived from the comparison of quasi-continuous measurements with parallel NOAA discrete air samples. We emphasize that this bias correction assumes that the bias remains constant during the inversion period (yearly for TM5) and, therefore, cannot correct for changes of the systematic bias on shorter time scales.

For validation, CH<sub>4</sub> measurements of discrete air samples from 3 European aircraft profile sites in Scotland, France, and Hungary are used, operated within the European CarboEurope project. The analyses of these samples were performed at LSCE, in the same manner as the RAMCES surface measurements.

### 3 Modelling

#### 3.1 Modelling protocol

The modelling protocol used in this study prescribed mainly the basic settings for the inversions, such as a priori emission inventories, observational data sets, time period, and requested model output. Atmospheric sinks were not prescribed. For both CH<sub>4</sub> and N<sub>2</sub>O, two types of inversions were performed: (1) the base inversions, S1–CH<sub>4</sub> and S1–N<sub>2</sub>O, respectively, using detailed bottom-up emission inventories for anthropogenic and natural sources as a priori emission estimates and (2) the “free inversions”, S2–CH<sub>4</sub> and S2–N<sub>2</sub>O, which do not use these bottom-up inventories. The objective of these “free inversions” is to explore the information content of the observations in the absence of detailed a priori information.

The CH<sub>4</sub> and N<sub>2</sub>O emission inventories applied in S1–CH<sub>4</sub> and S1–N<sub>2</sub>O are summarized in Tables 3 and 4, respectively. For the anthropogenic sources (except biomass burning), the EDGARv4.1 emission inventory for 2005 was used (as 2005 is the most recent available year in EDGARv4.1). For S2–CH<sub>4</sub> and S2–N<sub>2</sub>O, a homogenous

## Top-down estimates of European CH<sub>4</sub> and N<sub>2</sub>O emissions

P. Bergamaschi et al.

Title Page

Abstract

Introduction

Conclusions

References

Tables

Figures



Back

Close

Full Screen / Esc

Printer-friendly Version

Interactive Discussion





## Top-down estimates of European CH<sub>4</sub> and N<sub>2</sub>O emissions

P. Bergamaschi et al.

Title Page

Abstract

Introduction

Conclusions

References

Tables

Figures



Back

Close

Full Screen / Esc

Printer-friendly Version

Interactive Discussion



distribution of emissions over land and over the ocean was used as starting point for the optimization (i.e. a “weak a priori” for TM5-4DVAR and TM3-STILT), with global total CH<sub>4</sub> and N<sub>2</sub>O emissions over land and over the ocean, respectively, close to the total emissions over land and over the ocean of the detailed a priori inventories (Bergamaschi et al., 2010; Corazza et al., 2011), hence effectively limiting the emissions that can be attributed to the ocean. For the NAME-INV model, no separation was made between land and ocean. Moreover, the NAME-INV model started from random emission maps rather than a homogenous distribution of emissions. Inversions S2 were not performed for LMDZ-4DVAR.

For the European limited domain models NAME-INV and STILT, background CH<sub>4</sub> and N<sub>2</sub>O mixing ratios were calculated by TM5-4DVAR (for NAME-INV CH<sub>4</sub> and N<sub>2</sub>O inversions and STILT N<sub>2</sub>O inversions) and by TM3 (for STILT CH<sub>4</sub> inversions) following the two-step scheme of Rödenbeck et al. (2009).

All models used the same observational data set described in Sect. 2 (with the exception of a few stations which are outside the domain of the limited domain models). For the continuously operated monitoring stations in the boundary layer, measurements between 12:00 and 15:00 LT were assimilated, while for mountain sites night-time measurements (between 0:00 and 3:00 LT) were used (with the exception of the NAME-INV model that used observations at all times, but with local contributions excluded as in Manning et al., 2011).

For the N<sub>2</sub>O inversions, bias corrections for the N<sub>2</sub>O observations from different networks or institutes were calculated within the 4DVAR optimization of the TM5-4DVAR and LMDZ-4DVAR models, as described by Corazza et al. (2011). For NAME-INV and TM3-STILT, the bias corrections calculated by TM5-4DVAR (Table 7) were applied.

### 3.2 Atmospheric models

The atmospheric models used in this study are summarized in Table 2 and briefly described in the following.

### 3.2.1 TM5-4DVAR

The TM5-4DVAR inverse modelling system is described in detail by Meirink et al. (2008). It is based on the two-way nested atmospheric zoom model TM5 (Krol et al., 2005). In this study we apply the zooming with  $1^\circ \times 1^\circ$  resolution over Europe, while the global domain is simulated at a horizontal resolution of  $6^\circ$  (longitude)  $\times$   $4^\circ$  (latitude). TM5 is an offline transport model, driven by meteorological fields from the European Centre for Medium-Range Weather Forecasts (ECMWF) ERA-Interim re-analysis (Dee et al., 2011). The 4-dimensional variational (4DVAR) optimization technique minimizes iteratively a cost function using the adjoint of the tangent linear model and the m1qn3 algorithm for minimization (Gilbert and Lemaréchal, 1989). We apply a “semi-exponential” description of the probability density function for the a priori emissions to force the a posteriori emissions to remain positive (Bergamaschi et al., 2009, 2010). In inversion S1-CH<sub>4</sub>, 4 groups of CH<sub>4</sub> emissions are optimized independently: (1) wetlands, (2) rice, (3) biomass burning, and (4) all remaining sources (Bergamaschi et al., 2010), and for S1-N<sub>2</sub>O the following 4 groups of N<sub>2</sub>O emissions: (1) soil, (2) ocean, (3) biomass burning, and (4) all remaining emissions (Corazza et al., 2011). In S2-CH<sub>4</sub> and S2-N<sub>2</sub>O, only total emissions are optimized. We assume uncertainties of 100 % per grid cell and month for each source group and apply spatial correlation scale lengths of 200 km in S1-CH<sub>4</sub> and S1-N<sub>2</sub>O. In the “free inversions” S2-CH<sub>4</sub> and S2-N<sub>2</sub>O, smaller correlation scale lengths of 50 km, and larger uncertainties of 500 % per grid cell and month are used to give the inversion enough freedom to retrieve regional hot spots (Bergamaschi et al., 2010; Corazza et al., 2011). The temporal correlation time scales are set to zero for the source groups with significant seasonal variations, and 9.5 months for the “remaining” CH<sub>4</sub> and N<sub>2</sub>O sources (which include major anthropogenic sources that are assumed to have no or only small seasonal variations) in S1-CH<sub>4</sub> and S1-N<sub>2</sub>O, and 1 month for the total emissions optimized in S2-CH<sub>4</sub> and S2-N<sub>2</sub>O.

## Top-down estimates of European CH<sub>4</sub> and N<sub>2</sub>O emissions

P. Bergamaschi et al.

[Title Page](#)[Abstract](#)[Introduction](#)[Conclusions](#)[References](#)[Tables](#)[Figures](#)[Back](#)[Close](#)[Full Screen / Esc](#)[Printer-friendly Version](#)[Interactive Discussion](#)

The photochemical sinks of CH<sub>4</sub> (due to OH in the troposphere, and OH, Cl, and O(<sup>1</sup>D) in the stratosphere) are simulated as described in Bergamaschi et al. (2010). The stratospheric sinks of N<sub>2</sub>O (photolysis and reaction with excited oxygen O(<sup>1</sup>D)) are modelled as in Corazza et al. (2011).

The observations errors were set to 3 ppb for CH<sub>4</sub>, and 0.3 ppb for N<sub>2</sub>O. The model representation error is estimated as a function of local emissions and 3-D gradients of simulated mixing ratios (Bergamaschi et al., 2010), resulting in overall (combined measurement and model representation) errors in the range between 3 ppb and up to ~ 1 ppm for CH<sub>4</sub>, and between 0.3 ppb and up to several ppb for N<sub>2</sub>O. For the N<sub>2</sub>O inversions we optimize bias parameters for the N<sub>2</sub>O observations from different networks or institutes (see Table 7), as described by Corazza et al. (2011).

### 3.2.2 LMDZ-4DVAR

The LMDZ-4DVAR inverse modelling framework is based on the offline and adjoint models of the Laboratoire de Météorologie Dynamique, version 4 (LMDZ) general circulation model (Hourdin and Armengaud, 1999; Hourdin et al., 2006). The offline model is driven by archived fields of winds, convection mass fluxes, and planetary boundary layer (PBL) exchange coefficients that have been calculated in prior integrations of the complete general circulation model, which was nudged to ECMWF ERA-Interim winds (Dee et al., 2011). In this study, LMDZ is used with a zoom over Europe at a resolution of approximately 1.2° × 0.8° and decreasing resolution away from Europe to a maximum grid size of approximately 7.2° × 3.6°. LMDZ has 19 hybrid pressure levels in the vertical dimension. The optimal fluxes were found by solving the cost function using the adjoint model and the Lanczos algorithm for N<sub>2</sub>O and the m1qn3 algorithm for CH<sub>4</sub>.

Details about the inversion framework for CH<sub>4</sub> are given in Pison et al. (2009, 2013). Only the total net emissions of methane are optimized, at the resolution of the grid-cell for 8 day periods. Prior uncertainties in each grid-cell are set to 100 % of the maximum flux over the grid-cell and its eight neighbours (so as to allow for a misplacement of the sources). Correlation scale lengths are used to compute the extra-diagonal terms in

## Top-down estimates of European CH<sub>4</sub> and N<sub>2</sub>O emissions

P. Bergamaschi et al.

Title Page

Abstract

Introduction

Conclusions

References

Tables

Figures



Back

Close

Full Screen / Esc

Printer-friendly Version

Interactive Discussion



## Top-down estimates of European CH<sub>4</sub> and N<sub>2</sub>O emissions

P. Bergamaschi et al.

Title Page

Abstract

Introduction

Conclusions

References

Tables

Figures



Back

Close

Full Screen / Esc

Printer-friendly Version

Interactive Discussion



the error covariance matrix: they are set at 500 km on land and 1000 km on sea (land and sea are not correlated); there are no time correlations. The “observation” errors include the errors due to the transport model and to the representativity of the grid cell compared to the measurement (combined measurement and model error ranging between 3 ppb and up to 450 ppb). Note that the OH fields are inverted simultaneously to the methane emissions, with constraints from methyl-chloroform.

Details about the inversion framework for N<sub>2</sub>O can be found in Thompson et al. (2011). For N<sub>2</sub>O, only total emissions were optimized. Prior uncertainties in each grid-cell were set to 100 % and correlation scale lengths of 500 km over land, 1000 km over ocean, and 3 months were used to form the full error covariance matrix, which was subsequently scaled to be consistent with a global total uncertainty of 3 TgN yr<sup>-1</sup> (approximately 18%). The error of the N<sub>2</sub>O observations was set to 0.3 ppb. Model representation errors incorporated an estimate of aggregation error, i.e. distribution of emissions within the grid-cell (Bergamaschi et al., 2010), and horizontal advection errors (Rödenbeck et al., 2003), resulting in total model errors ranging from about 0.2 ppb to 1 ppb. In addition to the emissions, bias parameters for the N<sub>2</sub>O observations from different networks or institutes were optimized, similarly to TM5-4DVAR (Corazza et al., 2011).

### 3.2.3 TM3-STILT

In the Jena inversions, the coupled system TM3-STILT is used for regional-scale high-resolution inversions. TM3-STILT (Trusilova et al., 2010) is a combination of the coarse-grid global 3-dimensional atmospheric offline transport model TM3 (Heimann and Köerner, 2003) and the fine-scale regional Stochastic Time-Inverted Lagrangian Transport model STILT (Gerbig et al., 2003; Lin et al., 2003). The models are coupled using the two-step nesting scheme of Rödenbeck et al. (2009), which allows the use of completely independent models for the representation of the global and the regional transport. The variational inversion algorithm of the Jena inversion scheme, applied in the global as well as in the regional inversion step, is described in detail in Rödenbeck

## Top-down estimates of European CH<sub>4</sub> and N<sub>2</sub>O emissions

P. Bergamaschi et al.

Title Page

Abstract

Introduction

Conclusions

References

Tables

Figures



Back

Close

Full Screen / Esc

Printer-friendly Version

Interactive Discussion



(2005). In this study, the global transport model TM3 is used with a spatial resolution of  $4^\circ \times 5^\circ$  and 19 vertical levels. STILT is driven by meteorological fields from ECMWF operational analysis, used here with a spatial resolution of  $0.25^\circ \times 0.25^\circ$  and confined to the lowest 61 vertical layers. The regional TM3-STILT inversions are conducted in this study on a  $1^\circ \times 1^\circ$  horizontal resolution grid covering the greater part of Europe ( $12^\circ \text{W}$ – $35^\circ \text{E}$ ,  $35$ – $62^\circ \text{N}$ ). Regional inversion results for CH<sub>4</sub> were obtained directly by the TM3-STILT system. For the regional N<sub>2</sub>O inversions the same modular nesting technique is applied to couple STILT with a baseline provided by TM5-4DVAR (Bergamaschi et al., 2010; Corazza et al., 2011) and the regional inversion step is performed in the Jena inversion system. The latter combination is referred to as TM5-STILT in the presentation of the N<sub>2</sub>O inversion results. In all regional inversions we optimize the total emissions. Uncertainties of 100 % per grid cell and month, with a spatial correlation scale length of 600 km and a temporal correlation time scale of 1 month, are assumed in the regional S1–CH<sub>4</sub> and S1–N<sub>2</sub>O inversions. In both S2 inversions the uncertainties are set to 500 % with a correlation scale length of 60 km and correlation time scale of 1 month. The observations errors were set to 3 ppb for CH<sub>4</sub>, and 0.2 ppb for N<sub>2</sub>O. Model representation errors are assigned to the individual sites according to their location with respect to continental, remote or oceanic situations (Rödenbeck, 2005) resulting in overall (combined measurement and model representation) errors in the range of 10–30 ppb for CH<sub>4</sub>, and 0.8 and 2.4 ppb for N<sub>2</sub>O. For N<sub>2</sub>O the bias parameters estimated by TM5-4DVAR (see Table 7) are applied in the regional inversions.

### 3.2.4 NAME-INV

The NAME-INV inverse modelling system is described in Manning et al. (2011) using one station to estimate UK and Northern European emissions of various trace gases and in Athanassiadou et al. (2011) for multiple stations across Europe. The transport of CH<sub>4</sub> and N<sub>2</sub>O from sources to observations is performed using the UK Met Office Lagrangian model NAME (Jones et al., 2007). Thousands of particles are released from each measurement for each 2 h period in 2006 and 2007, and these are tracked

## Top-down estimates of European CH<sub>4</sub> and N<sub>2</sub>O emissions

P. Bergamaschi et al.

Title Page

Abstract

Introduction

Conclusions

References

Tables

Figures



Back

Close

Full Screen / Esc

Printer-friendly Version

Interactive Discussion



backwards in time over a period of 13 days (long enough for the majority of particles to leave the domain of interest). The 13 day time-integrated concentrations only include contributions from 0–100 m a.g.l.; representative of surface emissions. The meteorological fields needed to run NAME are from the global version of the Met Office Unified Model (UM) at a resolution of  $0.56^\circ \times 0.37^\circ$  and 31 vertical levels from surface to about 19 km (see Table 2). The domain used for the inversion extends from  $14.63^\circ$  W to  $39.13^\circ$  E and from  $33.81^\circ$  N to  $72.69^\circ$  N, with a resolution of  $0.42^\circ \times 0.27^\circ$  in the longitudinal and latitudinal directions respectively. The inversion is initialised either from the modelling protocol a priori, or from a random emissions field as in Manning et al. (2011). In the latter case, the cost function used in the optimization is the same as in Manning et al. (2011). In S1, when the inversion is initialised and guided by the a priori emission inventory, a modified version is used (original cost function + RMSE between modelled values and a priori). To account for the imbalance in the contribution from different grid boxes (i.e., the grids more distant from the observations are expected to contribute less than those that are closer), grid boxes are progressively grouped together into increasingly larger boxes as the individual contributions decrease.

In all inversions, the total annual emissions are optimised without any partitioning to various sectors. The background values used for CH<sub>4</sub> and N<sub>2</sub>O are from TM5-4DVAR following the two-step scheme of Rödenbeck et al. (2009). Observations at all times have been used (i.e., not only in the time windows specified in Sect. 3.1), but excluding local contributions (Manning et al., 2011). An estimate of the uncertainty in the emissions is obtained from the 5th and 95th percentiles of 52 independent inversion solutions (the mean of these being the final solution). The independent inversion solutions are considered to simulate uncertainties in the meteorology, dispersion and observations. For each inversion a different time series of random noise is applied to the observations. The random element at each observation is multiplicative and taken from a lognormal distribution with mean 1 and variance, arbitrarily, set to one fifth of the standard deviation of baseline observations about a smoothed baseline value as in



bottom-up respectively. Both approaches show coherently elevated CH<sub>4</sub> emissions over BENELUX/north-western Germany, and southern UK. The S2-CH<sub>4</sub> inversions also show somewhat elevated emissions per area in southern Poland, where large coal mines are located. However, the inversions are not able to reproduce the very pronounced CH<sub>4</sub> emission hotspot of the bottom-up inventory in this area. This is probably largely due to the limitations of the inversion's ability to resolve point sources accurately (also given the limitation of the sparse atmospheric measurement network) but could also point to a bottom-up overestimate of the CH<sub>4</sub> emissions from the coal mining in this area. In fact, the EDGARv4.2 estimate of CH<sub>4</sub> emissions from coal mines in Poland (1.71 Tg CH<sub>4</sub> yr<sup>-1</sup>) is about 4 times higher than that reported under UNFCCC (0.43 Tg CH<sub>4</sub> yr<sup>-1</sup>, see Table 6). However, it should be pointed out that the bottom-up emissions have large uncertainties, estimated to be 49 % for UNFCCC, and 83 % for EDGARv4.2 for the coal mines in Poland.

In the following discussion, we analyse the CH<sub>4</sub> emissions per country for those countries whose emissions are reasonably well constrained by the available observations. These are mainly north-western and eastern European countries (Fig. 3), while southern European countries are only poorly constrained. For smaller countries, we present aggregated emissions (e.g. BENELUX), as they are considered more robust than emissions of individual small countries. The normalized range of derived CH<sub>4</sub> emissions (defined as  $(E_{\max} - E_{\min}) / (E_{\max} + E_{\min})$ ) is between ±16 % and ±44 % for the analysed countries (or combined countries), and ±25 % for the total CH<sub>4</sub> emissions of all north-western and eastern European countries shown in Fig. 3 (inversion S1-CH<sub>4</sub>). For some countries, the range of emission estimates from all 4 models is close to the uncertainties estimated for the individual inversions (e.g. Poland), but there are also several countries with much larger emission ranges (e.g. France). This shows that there are systematic differences between the inversions, which are not covered by the uncertainty estimates of the individual inversions.

The country totals of the “free” inversion S2-CH<sub>4</sub> are in general very close to those of S1-CH<sub>4</sub> for most countries, demonstrating the strong observational constraints.

## Top-down estimates of European CH<sub>4</sub> and N<sub>2</sub>O emissions

P. Bergamaschi et al.

[Title Page](#)[Abstract](#)[Introduction](#)[Conclusions](#)[References](#)[Tables](#)[Figures](#)[Back](#)[Close](#)[Full Screen / Esc](#)[Printer-friendly Version](#)[Interactive Discussion](#)





emissions over land (in case of coastal grid cells the total emissions of this grid cell are attributed to the land). In contrast, previous NAME-INV inversion studies used different country masks, taking into account also offshore emissions at some further distance from the coastlines (Manning et al., 2011).

It is important to note that the inverse modelling estimates the total of the anthropogenic and natural emissions. According to the bottom-up inventories applied in our study, however, it is estimated that natural CH<sub>4</sub> emissions only play a minor role for the countries considered here (shown by the dash-dotted lines in Figs. 3 and 4). This is important when comparing the CH<sub>4</sub> emissions derived by the inverse models with anthropogenic CH<sub>4</sub> emissions reported to the UNFCCC (shown by black lines in Fig. 3). The range of CH<sub>4</sub> emissions estimated by the inverse models overlaps for most countries with the uncertainty range of the UNFCCC emissions. Nevertheless, there is a clear tendency to higher CH<sub>4</sub> emissions derived by 3 of the inverse models (TM5-4DVAR, LMDZ-4DVAR, TM3-STILT) compared to UNFCCC, while NAME-INV is in most cases close to UNFCCC. For comparing different approaches, realistic uncertainty estimates are essential to evaluate their consistency. Under the UNFCCC, European countries report uncertainty estimates for individual source categories, taking into account uncertainty estimates for activity data and for emission factors (both for CH<sub>4</sub> and for N<sub>2</sub>O usually the latter is the dominant term). Since uncertainties of total emissions are usually not reported, we estimate these assuming that the uncertainties of different IPCC/UNFCCC source categories are uncorrelated (but fully correlated for sub-categories). Furthermore, we assume correlated errors when aggregating individual source categories from different countries (as different countries usually apply similar approaches). Table 6 shows the UNFCCC uncertainty estimates for the 6 major CH<sub>4</sub> source categories and our derived estimates of the total uncertainty per country (and aggregated countries). Overall the estimated total uncertainties are surprisingly low, between 17 and 26 % for the countries considered and about 20 % for the total CH<sub>4</sub> emissions of all north-western and eastern European countries.

## Top-down estimates of European CH<sub>4</sub> and N<sub>2</sub>O emissions

P. Bergamaschi et al.

[Title Page](#)[Abstract](#)[Introduction](#)[Conclusions](#)[References](#)[Tables](#)[Figures](#)[Back](#)[Close](#)[Full Screen / Esc](#)[Printer-friendly Version](#)[Interactive Discussion](#)

**Top-down estimates  
of European CH<sub>4</sub> and  
N<sub>2</sub>O emissions**

P. Bergamaschi et al.

Title Page

Abstract

Introduction

Conclusions

References

Tables

Figures



Back

Close

Full Screen / Esc

Printer-friendly Version

Interactive Discussion



Table 6 also includes the CH<sub>4</sub> emission estimates from EDGARv4.1 for 2005 (used as a priori in the inversion) and EDGARv4.2 for 2006–2007 (which became available after completion of the inversions in this study). Overall the numbers for EDGARv4.1 (2005) and EDGARv4.2 for 2006–2007 are very similar (total of north-western and eastern European countries (denoted “NWE+NEE”): 16.0 Tg CH<sub>4</sub> yr<sup>-1</sup> and 15.6 Tg CH<sub>4</sub> yr<sup>-1</sup>, respectively); smaller differences are due to several updates in EDGARv4.2 and to small trends between 2005 and 2006–2007. Comparison of UNFCCC emissions with EDGARv4.2 shows overall good consistency for enteric fermentation, manure management, and solid waste, for which the EDGARv4.2 estimates are for most countries within the uncertainty range of the UNFCCC emissions (Table 6). However, there are considerable differences in particular for solid fuels (i.e. coal mining) and oil and natural gas, for which EDGARv4.2 estimates 1.4 Tg CH<sub>4</sub> yr<sup>-1</sup> and 1.9 Tg CH<sub>4</sub> yr<sup>-1</sup>, respectively, higher emissions for the NWE+NEE total than UNFCCC. For single countries, the largest differences are for solid fuels from Poland (EDGARv4.2: 1.71 (0.29–3.21) Tg CH<sub>4</sub> yr<sup>-1</sup>; UNFCCC: 0.43 (0.22–0.64) Tg CH<sub>4</sub> yr<sup>-1</sup>) and oil and natural gas from France (EDGARv4.2: 1.49 Tg CH<sub>4</sub> yr<sup>-1</sup>; UNFCCC: 0.05 (0.04–0.06) Tg CH<sub>4</sub> yr<sup>-1</sup>). Since uncertainty estimates are not standardly available for each sector and country in EDGARv4.2, a strict comparison cannot be made. However, the large differences between the two bottom-up estimates highlight the large uncertainties for fugitive emissions related to production (and transmission/distribution) of fossil fuels.

For TM5-4DVAR, LMDZ-4DVAR, and TM3-STILT, the derived emissions are in general closer to the total emissions from EDGARv4.2 than those from UNFCCC, while NAME-INV, as already mentioned, is relatively close to UNFCCC.

Our inverse modelling estimates of the total emissions per country do not account for offshore emissions. According to EDGARv4.2 about 0.8 Tg CH<sub>4</sub> yr<sup>-1</sup> are emitted offshore over the European seas (mainly from oil and gas production), while natural CH<sub>4</sub> emissions of about 0.4 Tg CH<sub>4</sub> yr<sup>-1</sup> over the European seas are estimated from our bottom-up inventories (total between 35° and 62° N and between 12° W and 35° E; see

Fig. 4). For comparison, Bange (2006) estimates natural CH<sub>4</sub> emissions from European coastal areas to be in the range 0.5 to 1.0 Tg CH<sub>4</sub> yr<sup>-1</sup> (including the Arctic Ocean, Baltic Sea, North Sea, northeastern Atlantic Ocean, Mediterranean Sea, and Black Sea).

The statistics of the assimilated observations are summarized in Fig. 5. Overall, all the models show relatively similar performance, with an average correlation coefficient between 0.7 and 0.8 and an average root mean square (RMS) difference between observed and assimilated CH<sub>4</sub> mixing ratios between ~ 25 and ~ 35 ppb.

All models have been validated against regular aircraft profiles performed within the CarboEurope project at 3 European monitoring sites (Fig. 6). These aircraft data have not been used in the inversion. However, for 2 aircraft sites (Griffin, Scotland and Hegyhatsal, Hungary) the corresponding surface observations have been assimilated (tall towers Angus (TT1) and Hegyhatsal (HU1)), while the surface observations at Orléans (France) were not used (since they started only in 2007), but the observations from Gif-sur-Yvette, about 100 km north of Orléans, were included. Hence, while surface mixing ratios are well constrained at these 3 aircraft sites, the comparison of observed and modelled vertical gradients allows the model-simulated vertical transport to be validated, which is of critical importance to the inversions. Figure 6 shows that all models reproduce the average observed vertical gradient in the lower troposphere relatively well, indicating overall realistic vertical mixing.

## 4.2 Inverse modelling of European N<sub>2</sub>O emission

Figures 7 and 8 show maps of derived N<sub>2</sub>O emissions (average 2006–2007) for inversions S1–N<sub>2</sub>O and S2–N<sub>2</sub>O, respectively. European N<sub>2</sub>O emissions are dominated by agricultural soils. Furthermore, N<sub>2</sub>O emissions from the chemical industry represent strong point sources, which are clearly visible in the a priori emission inventory.

In general, the 4 models show a relatively consistent picture for S1–N<sub>2</sub>O, with moderate N<sub>2</sub>O emission increments on larger regional scales, while largely preserving the spatial “fine-structure” of the a priori emission inventory. As for S1–CH<sub>4</sub>, however,

## Top-down estimates of European CH<sub>4</sub> and N<sub>2</sub>O emissions

P. Bergamaschi et al.

Title Page

Abstract

Introduction

Conclusions

References

Tables

Figures



Back

Close

Full Screen / Esc

Printer-friendly Version

Interactive Discussion





## Top-down estimates of European CH<sub>4</sub> and N<sub>2</sub>O emissions

P. Bergamaschi et al.

Title Page

Abstract

Introduction

Conclusions

References

Tables

Figures



Back

Close

Full Screen / Esc

Printer-friendly Version

Interactive Discussion



assuming zero emissions for the specific category as the lowermost boundary for any relative error larger than 100 %. Figure 9 shows that the range of the inverse modelling estimates is much smaller than the UNFCCC uncertainty range for most countries (including the total emissions from north-western and eastern Europe). This finding is consistent with the analysis of error statistics of bottom-up inventories by Leip (2010), suggesting that the current UNFCCC uncertainty estimates of N<sub>2</sub>O bottom-up emission inventories are likely overestimated.

It is important to note, however, that significant biases in N<sub>2</sub>O measurements exist between different laboratories that require corrections (Table 7). The bias corrections calculated by TM5-4DVAR and LMDZ-4DVAR are within ~0.3 ppb compared to the bias determined for those stations for which parallel NOAA flask measurements are available (for stations with at least 10 coinciding hourly measurements per year). This is somewhat worse than the agreement of 0.1–0.2 ppb reported by Corazza et al. (2011) and may indicate some limitations of the applied bias correction scheme, which does not account for potential changes of the bias within the inversion period (TM5-4DVAR: 1 year, LMDZ-4DVAR: 2 years).

Figure 11 shows the correlation coefficients and RMS differences between (bias-corrected) observed and simulated N<sub>2</sub>O mixing ratios at the monitoring stations used in inversion S1–N<sub>2</sub>O. The mean correlation coefficients for the 4 models are in the range between 0.6 and 0.7 (averaged over all stations), which is somewhat lower than for CH<sub>4</sub> (average correlation coefficients between 0.7 and 0.8; Fig. 5). This is probably mainly due to the lower atmospheric N<sub>2</sub>O variability compared to CH<sub>4</sub>, but may be partly also due to the mentioned limitations of the quality of the N<sub>2</sub>O data.

## 5 Conclusions

We estimated European CH<sub>4</sub> and N<sub>2</sub>O emissions for 2006 and 2007 using four independent inverse modelling systems that were constrained by quasi-continuous observations from various European monitoring stations (including five tall towers),

## Top-down estimates of European CH<sub>4</sub> and N<sub>2</sub>O emissions

P. Bergamaschi et al.

Title Page

Abstract

Introduction

Conclusions

References

Tables

Figures



Back

Close

Full Screen / Esc

Printer-friendly Version

Interactive Discussion



complemented by further European and global discrete air sampling sites. Although the range of CH<sub>4</sub> emissions estimated by the inverse models overlaps for most countries with the uncertainty range of the UNFCCC emissions, 3 of 4 models show a clear tendency to higher emissions compared to the anthropogenic emissions reported under UNFCCC for the total of north-western and eastern European countries (range of TM5-4DVAR, LMDZ-4DVAR, and TM3-STILT after correction for natural sources 26–56 % higher than UNFCCC), while NAME-INV yields estimates of country totals very close to UNFCCC. This analysis suggests that (1) CH<sub>4</sub> emissions reported to UNFCCC could be underestimated for some of the European countries analysed in this study or (2) natural CH<sub>4</sub> emissions are underestimated, or (3) atmospheric models may have significant biases. Although the flux inversions do not allow direct conclusions about specific source categories, the comparison between UNFCCC and EDGARv4.2 shows the critical importance of fugitive emissions from fossil fuels (coal mining, oil production, and production, transmission, and distribution of natural gas) for which large differences are apparent between UNFCCC and EDGARv4.2 inventories, outside the estimated UNFCCC uncertainties for some countries. In addition, it is also important that natural CH<sub>4</sub> emissions are better quantified in the future, especially CH<sub>4</sub> from wetlands and wet soils. Isotope analysis ( $\delta^{13}\text{C}$  and  $\delta\text{D}$ ) could provide some additional information of the relative contribution of different sources; however the constraints on the European scale might be limited by overlapping isotopic signatures of the sources.

Furthermore, the transport models need better validation. Although the presented validation against independent aircraft CH<sub>4</sub> observations suggests vertical mixing is realistically modelled overall, we emphasize the need to extend this validation to more sites and to include further diagnostics such as <sup>222</sup>Rn and boundary layer height dynamics. These are currently being investigated in more detail in the framework of the InGOS (“Integrated non-CO<sub>2</sub> Greenhouse gas Observing System”; <http://www.ingos-infrastructure.eu/>) project.

The N<sub>2</sub>O emissions derived by the inverse models are in general very close to the UNFCCC values, with the range of the inverse modelling estimates being much smaller





## References

- Aalto, T., Hatakka, J., and Lallo, M.: Tropospheric methane in northern Finland: seasonal variations, transport patterns and correlations with other trace gases, *Tellus B*, 59, 251–259, 2007.
- 5 Athanassiadou, M., Manning, A. J., and Bergamaschi, P.: The NAME-inversion method in the nitro Europe project, in: 14th Conference on Harmonisation within Atmospheric Dispersion Modelling for Regulatory Purposes, 2–6 October 2011, Kos, Greece, available at: [http://www.harmo.org/Conferences/Proceedings/\\_Kos/publishedSections/H14-248.pdf](http://www.harmo.org/Conferences/Proceedings/_Kos/publishedSections/H14-248.pdf) (last access: 13 June 2014), H14–248, 627–631, 2011.
- 10 Bange, H. W.: Nitrous oxide and methane in European coastal waters, *Estuar. Coast. Shelf S.*, 70, 361–374, 2006.
- Barnes, J. and Upstill-Goddard, R. C.: N<sub>2</sub>O seasonal distributions and air–sea exchange in UK estuaries: implications for the tropospheric N<sub>2</sub>O source from European coastal waters, *J. Geophys. Res.*, 116, G01006, doi:10.1029/2009JG001156, 2011.
- 15 Bergamaschi, P. (Ed.): Atmospheric Monitoring and Inverse Modelling for Verification of National and EU Bottom-up GHG Inventories – report of the workshop “Atmospheric Monitoring and Inverse Modelling for Verification of National and EU Bottom-up GHG Inventories” under the mandate of Climate Change Committee Working Group I, Casa Don Guanella, Ispra, Italy (8–9 March 2007), 153 pp., European Commission Joint Research Centre, Institute for Environment and Sustainability, 2007.
- 20 Bergamaschi, P., Frankenberg, C., Meirink, J. F., Krol, M., Dentener, F., Wagner, T., Platt, U., Kaplan, J. O., Körner, S., Heimann, M., Dlugokencky, E. J., and Goede, A.: Satellite cartography of atmospheric methane from SCIAMACHY onboard ENVISAT: 2. Evaluation based on inverse model simulations, *J. Geophys. Res.*, 112, D02304, doi:10.1029/2006JD007268, 2007.
- 25 Bergamaschi, P., Frankenberg, C., Meirink, J. F., Krol, M., Villani, M. G., Houweling, S., Dentener, F., Dlugokencky, E. J., Miller, J. B., Gatti, L. V., Engel, A., and Levin, I.: Inverse modeling of global and regional CH<sub>4</sub> emissions using SCIAMACHY satellite retrievals, *J. Geophys. Res.*, 114, D22301, doi:10.1029/2009JD012287, 2009.
- 30 Bergamaschi, P., Krol, M., Meirink, J. F., Dentener, F., Segers, A., van Aardenne, J., Monni, S., Vermeulen, A., Schmidt, M., Ramonet, M., Yver, C., Meinhardt, F., Nisbet, E. G., Fisher,

ACPD

14, 15683–15734, 2014

### Top-down estimates of European CH<sub>4</sub> and N<sub>2</sub>O emissions

P. Bergamaschi et al.

Title Page

Abstract

Introduction

Conclusions

References

Tables

Figures



Back

Close

Full Screen / Esc

Printer-friendly Version

Interactive Discussion



## Top-down estimates of European CH<sub>4</sub> and N<sub>2</sub>O emissions

P. Bergamaschi et al.

Title Page

Abstract

Introduction

Conclusions

References

Tables

Figures



Back

Close

Full Screen / Esc

Printer-friendly Version

Interactive Discussion



- R., O'Doherty, S., and Dlugokencky, E. J.: Inverse modeling of European CH<sub>4</sub> emissions 2001–2006, *J. Geophys. Res.*, 115, D22309, doi:10.1029/2010JD014180, 2010.
- Bergamaschi, P., Houweling, S., Segers, A., Krol, M., Frankenberg, C., Scheepmaker, R. A., Dlugokencky, E., Wofsy, S., Kort, E., Sweeney, C., Schuck, T., Brenninkmeijer, C., Chen, H., Beck, V., and Gerbig, C.: Atmospheric CH<sub>4</sub> in the first decade of the 21st century: inverse modeling analysis using SCIAMACHY satellite retrievals and NOAA surface measurements, *J. Geophys. Res.*, 118, 7350–7369, doi:10.1002/jgrd.50480, 2013.
- Bousquet, P., Ciais, P., Miller, J. B., Dlugokencky, E. J., Hauglustaine, D. A., Prigent, C., Van der Werf, G. R., Peylin, P., Brunke, E.-G., Carouge, C., Langenfelds, R. L., Lathière, J., Papa, F., Ramonet, M., Schmidt, M., Steele, L. P., Tyler, S. C., and White, J.: Contribution of anthropogenic and natural sources to atmospheric methane variability, *Nature*, 443, 439–443, doi:10.1038/nature05132, 2006.
- Bouwman, A. F., Van der Hoek, K. W., and Olivier, J. G. J.: Uncertainties in the global source distribution of nitrous oxide, *J. Geophys. Res.*, 100, 2785–2800, 1995.
- Corazza, M., Bergamaschi, P., Vermeulen, A. T., Aalto, T., Haszpra, L., Meinhardt, F., O'Doherty, S., Thompson, R., Moncrieff, J., Popa, E., Steinbacher, M., Jordan, A., Dlugokencky, E., Brühl, C., Krol, M., and Dentener, F.: Inverse modelling of European N<sub>2</sub>O emissions: assimilating observations from different networks, *Atmos. Chem. Phys.*, 11, 2381–2398, doi:10.5194/acp-11-2381-2011, 2011.
- Cunnold, D. M., Steele, L. P., Fraser, P. J., Simmonds, P. G., Prinn, R. G., Weiss, R. F., Porter, L. W., O'Doherty, S., Langenfelds, R. L., Krummel, P. B., Wang, H. J., Emmons, L., Tie, X. X., Dlugokencky, E. J.: In situ measurements of atmospheric methane at GAGE/AGAGE sites during 1985–2000 and resulting inferences, *J. Geophys. Res.*, 107, 4225, doi:10.1029/2001JD001226, 2002.
- Dee, D. P., Uppala, S. M., Simmons, A. J., Berrisford, P., Poli, P., Kobayashi, S., Andrae, U., Balmaseda, M. A., Balsamo, G., Bauer, P., Bechtold, P., Beljaars, A. C. M., van de Berg, L., Bidlot, J., Bormann, N., Delsol, C., Dragani, R., Fuentes, M., Geer, A. J., Haimberger, L., Healy, S. B., Hersbach, H., Holm, E. V., Isaksen, I., Kållberg, P., Köhler, M., Matricardi, M., McNally, A. P., Monge-Sanz, B. M., Morcrette, J.-J., Park, B.-K., Peubey, C., de Rosnay, P., Tavolato, C., Thepaut, J.-N., and Vitart, F.: The ERA-Interim reanalysis: configuration and performance of the data assimilation system, *Q. J. Roy. Meteor. Soc.*, 137, 553–597, 2011.
- Dlugokencky, E. J., Steele, L. P., Lang, P. M., and Masarie, K. A.: The growth rate and distribution of atmospheric methane, *J. Geophys. Res.*, 99, 17021–17043, 1994.

**Top-down estimates  
of European CH<sub>4</sub> and  
N<sub>2</sub>O emissions**

P. Bergamaschi et al.

Title Page

Abstract

Introduction

Conclusions

References

Tables

Figures



Back

Close

Full Screen / Esc

Printer-friendly Version

Interactive Discussion



Dlugokencky, E. J., Houweling, S., Bruhwiler, L., Masarie, K. A., Lang, P. M., Miller, J. B., and Tans, P. P.: Atmospheric methane levels off: temporary pause or a new steady-state?, *Geophys. Res. Lett.*, 30, 1992, doi:10.1029/2003GL018126, 2003.

5 Dlugokencky, E. J., Myers, R. C., Lang, P. M., Masarie, K. A., Crotwell, A. M., Thoning, K. W., Hall, B. D., Elkins, J. W., and Steele, L. P.: Conversion of NOAA atmospheric dry air CH<sub>4</sub> mole fractions to a gravimetrically prepared standard scale, *J. Geophys. Res.*, 110, D18306, doi:10.1029/2005JD006035, 2005.

10 Dlugokencky, E. J., Bruhwiler, L., White, J. W. C., Emmons, L. K., Novelli, P. C., Montzka, S. A., Masarie, K. A., Lang, P. M., Crotwell, A. M., Miller, J. B., and Gatti, L. V.: Observational constraints on recent increases in the atmospheric CH<sub>4</sub> burden, *Geophys. Res. Lett.*, 36, L18803, doi:10.1029/2009GL039780, 2009.

EEA: Annual European Union greenhouse gas inventory 1990–2011 and inventory report 2013, EEA Technical report No 8/2013, European Commission, DG Climate Action and European Environment Agency, available at: <http://www.eea.europa.eu/publications/european-union-greenhouse-gas-inventory-2013> (last access: 13 June 2014), 2013.

15 Forster, P., Ramaswamy, V., Artaxo, P., Berntsen, T., Betts, R., Fahey, D. W., Haywood, J., Lean, J., Lowe, D. C., Myhre, G., Nganga, J., Prinn, R., Raga, G., Schulz, M., and Van Dorland, R.: Changes in atmospheric constituents and in radiative forcing, in: *Climate Change 2007: The Physical Science Basis. Contribution of Working Group I to the Fourth Assessment Report of the Intergovernmental Panel on Climate Change*, edited by: Solomon, S., Qin, D., Manning, M., Chen, Z., Marquis, M., Averyt, K. B., Tignor, M., and Miller, H. L., Cambridge University Press, Cambridge, UK and New York, NY, USA, 2007.

20 Gerbig, C., Lin, J., Wofsy, S., Daube, B., Andrews, A., Stephens, B., Bakwin, P., and C. Grainger: Toward constraining regional-scale fluxes of CO<sub>2</sub> with atmospheric observations over a continent: 2. Analysis of COBRA data using a receptor-oriented framework, *J. Geophys. Res.*, 108, 4757, doi:10.1029/2003JD003770, 2003.

Gilbert, J. C. and Lemaréchal, C.: Some numerical experiments with variable-storage quasi-Newton algorithms, *Mathematical Programming, Math. Programm.*, 45, 407–435, 1989.

25 Hall, B. D., Dutton, G. S., and Elkins, J. W.: The NOAA nitrous oxide standard scale for atmospheric observations, *J. Geophys. Res.*, 112, D09305, doi:10.1029/2006JD007954, 2007.

30 Heimann, M. and Koerner, S.: The Global Atmospheric Tracer Model TM3, Tech. Rep. 5 Rep., Max Planck Institute for Biogeochemistry (MPI-BGC), Jena, Germany, 2003.

## Top-down estimates of European CH<sub>4</sub> and N<sub>2</sub>O emissions

P. Bergamaschi et al.

Title Page

Abstract

Introduction

Conclusions

References

Tables

Figures



Back

Close

Full Screen / Esc

Printer-friendly Version

Interactive Discussion



- Hein, R., Crutzen, P. J., and Heimann, M.: An inverse modeling approach to investigate the global atmospheric methane cycle, *Global Biogeochem. Cy.*, 11, 43–76, 1997.
- Hirsch, A. I., Michalak, A. M., Bruhwiler, L. M., Peters, W., Dlugokencky, E. J., and Tans, P. P.: Inverse modeling estimates of the global nitrous oxide surface flux from 1998–2001, *Global Biogeochem. Cy.*, 20, GB1008, doi:10.1029/2004GB002443, 2006.
- Hourdin, F. and Armengaud, A.: The use of finite-volume methods for atmospheric advection of trace species, Part I: Test of various formulations in a general circulation model, *Mon. Weather Rev.*, 127, 822–837, 1999.
- Hourdin, F., Musat, I., Bony, S., Braconnot, P., Codron, F., Dufresne, J.-L., Fairhead, L., Filiberti, M.-A., Friedlingstein, P., Grandpeix, J.-Y., Krinner, G., Le Van, P., Li, Z.-X., and Lott, F.: The LMDZ4 general circulation model: climate performance and sensitivity to parameterized physics with emphasis on tropical convection, *Clim. Dynam.*, 27, 787–813, 2006.
- Houweling, S., Kaminski, T., Dentener, F., Lelieveld, J., and Heimann, M.: Inverse modeling of methane sources and sinks using the adjoint of a global transport model, *J. Geophys. Res.*, 104, 26137–26160, 1999.
- Huang, J., Golombek, A., Prinn, R., Weiss, R., Fraser, P., Simmonds, P., Dlugokencky, E. J., Hall, B., Elkins, J., Steele, P., Langenfelds, R., Krummel, P., Dutton, G., and Porter, L.: Estimation of regional emissions of nitrous oxide from 1997 to 2005 using multinet network measurements, a chemical transport model, and an inverse method, *J. Geophys. Res.*, 113, D17313, doi:10.1029/2007JD009381, 2008.
- IPCC: 2006 IPCC Guidelines for National Greenhouse Gas Inventories, Prepared by the National Greenhouse Gas Inventories Programme Institute for Global Environmental Strategies, Japan, available at: [http://www.ipcc-nggip.iges.or.jp/public/2006gl/pdf/0\\_Overview/V0\\_0\\_Cover.pdf](http://www.ipcc-nggip.iges.or.jp/public/2006gl/pdf/0_Overview/V0_0_Cover.pdf) (last access: 13 June 2014), 2006.
- Jones, A. R., Thomson, D. J., Hort, M., and Devenish, B.: The U. K. Met Office's next-generation atmospheric dispersion model, NAME III, in: *Proceedings of the 27th NATO/CCMS International Technical Meeting on Air Pollution Modelling and its Application*, edited by: Borrego, C. and Norman, A. L., 580–589, Springer, available at: [http://link.springer.com/chapter/10.1007/978-0-387-68854-1\\_62#page-2](http://link.springer.com/chapter/10.1007/978-0-387-68854-1_62#page-2) (last access: 13 June 2014), 2007.
- Karion, A., Sweeney, C., Pétron, G., Frost, G., Hardesty, R. M., Kofler, J., Miller, B. R., Newberger, T., Wolter, S., Banta, R., Brewer, A., Dlugokencky, E., Lang, P. M., Montzka, S. A., Schnell, R., Tans, P., Trainer, M., Zamora, R., and Conley, S.: Methane emissions estimate

**Top-down estimates  
of European CH<sub>4</sub> and  
N<sub>2</sub>O emissions**

P. Bergamaschi et al.

[Title Page](#)[Abstract](#)[Introduction](#)[Conclusions](#)[References](#)[Tables](#)[Figures](#)[Back](#)[Close](#)[Full Screen / Esc](#)[Printer-friendly Version](#)[Interactive Discussion](#)

from airborne measurements over a western United States natural gas field, *Geophys. Res. Lett.*, 40, 1–5, 2013.

Kirschke, S., Bousquet, P., Ciais, P., Saunoy, M., Canadell, J. G., Dlugokencky, E. J., Bergamaschi, P., Bergmann, D., Blake, D. R., Bruhwiler, L., Cameron-Smith, P., Castaldi, S., Chevallier, F., Feng, L., Fraser, A., Heimann, M., Hodson, E. L., Houweling, S., Josse, B., Fraser, P. J., Krummel, P. B., Lamarque, J.-F., Langenfelds, R. L., Le Quééré, C., Naik, V., O'Doherty, S., Palmer, P. I., Pison, I., Plummer, D., Poulter, B., Prinn, R. J., Rigby, M., Ringeval, B., Santini, M., Schmidt, M., Shindell, D. T., Simpson, I. J., Spahni, R., Steele, L. P., Strode, S. A., Sudo, K., Szopa, S., van der Werf, G. R., Voulgarakis, A., van Weele, M., Weiss, R. F., Williams, J. E., and Zeng, G.: Three decades of global methane sources and sinks, *Nat. Geosci.*, 6, 813–823, 2013.

Kort, E. A., Eluszkiewicz, J., Stephens, B. B., Miller, J. B., Gerbig, C., Nehr Korn, T., D. B. C., Kaplan, J. O., Houweling, S., and Wofsy, S. C.: Emissions of CH<sub>4</sub> and N<sub>2</sub>O over the United States and Canada based on a receptor-oriented modeling framework and COBRA-NA atmospheric observations, *Geophys. Res. Lett.*, 35, L18808, doi:10.1029/2008GL034031, 2008.

Krol, M., Houweling, S., Bregman, B., van den Broek, M., Segers, A., van Velthoven, P., Peters, W., Dentener, F., and Bergamaschi, P.: The two-way nested global chemistry-transport zoom model TM5: algorithm and applications, *Atmos. Chem. Phys.*, 5, 417–432, doi:10.5194/acp-5-417-2005, 2005.

Lambert, G. and Schmidt, S.: Reevaluation of the oceanic flux of methane: uncertainties and long term variations, *Chemosphere*, 26, 579–589, 1993.

Leip, A.: Quantitative quality assessment of the greenhouse gas inventory for agriculture in Europe, *Climatic Change*, 103, 245–261, 2010.

Leip, A., Busto, M., Corazza, M., Bergamaschi, P., Koeble, R., Dechow, R., Monni, S., and de Vries, W.: Estimation of N<sub>2</sub>O fluxes at the regional scale: data, models, challenges, *Current Opinion in Environmental Sustainability*, 3, 1–11, 2011.

Lin, J. C., Gerbig, C., Wofsy, S. C., Andrews, A. E., Daube, B. C., Davis, K. J., and Grainger, C. A.: A near-field tool for simulating the upstream influence of atmospheric observations: the Stochastic Time-Inverted Lagrangian Transport (STILT) model, *J. Geophys. Res.*, 108, 4493, doi:10.1029/2002JD003161, 2003.

**Top-down estimates  
of European CH<sub>4</sub> and  
N<sub>2</sub>O emissions**

P. Bergamaschi et al.

Title Page

Abstract

Introduction

Conclusions

References

Tables

Figures



Back

Close

Full Screen / Esc

Printer-friendly Version

Interactive Discussion



Liss, P. S. and Merlivat, L.: Air–sea exchange rates: introduction and synthesis, in: *The Role of Air–Sea Exchange in Geochemical Cycling*, edited by: Buat-Menard, P., Reidel Publishing Company, Dordrecht, 113–127, 1986.

Manning, A. J., O'Doherty, S., Jones, A. R., Simmonds, P. G., and Derwent, R. G.: Estimating UK methane and nitrous oxide emissions from 1990 to 2007 using an inversion modeling approach, *J. Geophys. Res.*, 116, D02305, doi:10.1029/2010JD014763, 2011.

Meirink, J. F., Bergamaschi, P., and Krol, M. C.: Four-dimensional variational data assimilation for inverse modelling of atmospheric methane emissions: method and comparison with synthesis inversion, *Atmos. Chem. Phys.*, 8, 6341–6353, doi:10.5194/acp-8-6341-2008, 2008.

Mikaloff Fletcher, S. E., Tans, P. P., Bruhwiler, L. M., Miller, J. B., and Heimann, M.: CH<sub>4</sub> sources estimated from atmospheric observations of CH<sub>4</sub> and its <sup>13</sup>C/<sup>12</sup>C isotopic ratios: 2. Inverse modelling of CH<sub>4</sub> fluxes from geographical regions, *Global Biogeochem. Cy.*, 18, GB4005, doi:10.1029/2004GB002224, 2004a.

Mikaloff Fletcher, S. E., Tans, P. P., Bruhwiler, L. M., Miller, J. B., and Heimann, M.: CH<sub>4</sub> sources estimated from atmospheric observations of CH<sub>4</sub> and its <sup>13</sup>C/<sup>12</sup>C isotopic ratios: 1. Inverse modelling of source processes, *Global Biogeochem. Cy.*, 18, GB4004, doi:10.1029/2004GB002223, 2004b.

Myhre, G., Shindell, D., Bréon, F.-M., Collins, W., Fuglestedt, J., Huang, J., Koch, D., Lamarque, J.-F., Lee, D., Mendoza, B., Nakajima, T., Robock, A., Stephens, G., Takemura, T., and Zhang, H.: Anthropogenic and Natural Radiative Forcing, in *Climate Change 2013: The Physical Science Basis. Contribution of Working Group I to the Fifth Assessment Report of the Intergovernmental Panel on Climate Change*, edited by: Stocker, T. F., Qin, D., Plattner, G.-K., Tignor, M., Allen, S. K., Boschung, J., Nauels, A., Xia, Y., Bex, V., and Midgley, P. M., Cambridge University Press, Cambridge, UK and New York, NY, USA, 2013.

Peylin, P., Law, R. M., Gurney, K. R., Chevallier, F., Jacobson, A. R., Maki, T., Niwa, Y., Patra, P. K., Peters, W., Rayner, P. J., Rödenbeck, C., van der Laan-Luijkx, I. T., and Zhang, X.: Global atmospheric carbon budget: results from an ensemble of atmospheric CO<sub>2</sub> inversions, *Biogeosciences*, 10, 6699–6720, doi:10.5194/bg-10-6699-2013, 2013.

Pison, I., Bousquet, P., Chevallier, F., Szopa, S., and Hauglustaine, D.: Multi-species inversion of CH<sub>4</sub>, CO and H<sub>2</sub> emissions from surface measurements, *Atmos. Chem. Phys.*, 9, 5281–5297, doi:10.5194/acp-9-5281-2009, 2009.

**Top-down estimates  
of European CH<sub>4</sub> and  
N<sub>2</sub>O emissions**

P. Bergamaschi et al.

Title Page

Abstract

Introduction

Conclusions

References

Tables

Figures



Back

Close

Full Screen / Esc

Printer-friendly Version

Interactive Discussion



Pison, I., Ringeval, B., Bousquet, P., Prigent, C., and Papa, F.: Stable atmospheric methane in the 2000s: key-role of emissions from natural wetlands, *Atmos. Chem. Phys.*, 13, 11609–11623, doi:10.5194/acp-13-11609-2013, 2013.

5 Popa, M. E., Gloor, M., Manning, A. C., Jordan, A., Schultz, U., Haensel, F., Seifert, T., and Heimann, M.: Measurements of greenhouse gases and related tracers at Bialystok tall tower station in Poland, *Atmos. Meas. Tech.*, 3, 407–427, doi:10.5194/amt-3-407-2010, 2010.

Prather, M. J., Holmes, C. D., and Hsu, J.: Reactive greenhouse gas scenarios: systematic exploration of uncertainties and the role of atmospheric chemistry, *Geophys. Res. Lett.*, 39, L09803, doi:10.1029/2012GL051440, 2012.

10 Prinn, R. G., Weiss, R. F., Fraser, P. J., Simmonds, P. G., Cunnold, D. M., Alyea, F. N., O'Doherty, S., Salameh, P., Miller, B. R., Huang, J., Wang, R. H. J., Hartley, D. E., Harth, C., Steele, L. P., Sturrock, G., Midgely, P. M., and McCulloch, A.: A history of chemically and radiatively important gases in air deduced from ALE/GAGE/AGAGE, *J. Geophys. Res.*, 115, 17751–17792, 2000.

15 Ravishankara, A. R., Daniel, J. S., and Portmann, R. W.: Nitrous oxide (N<sub>2</sub>O): the dominant ozone-depleting substance emitted in the 21st century, *Science*, 326, 123–125, 2009.

Ridgwell, A. J., Marshall, S. J., and Gregson, K.: Consumption of atmospheric methane by soils: a process-based model, *Global Biogeochem. Cy.*, 13, 59–70, doi:10.1029/1998GB900004, 1999.

20 Rigby, M., Prinn, R. G., Fraser, P. J., Simmonds, P. G., Langenfelds, R. L., Huang, J., Cunnold, D. M., Steele, L. P., Krummel, P. B., Weiss, R. F., O'Doherty, S., Salameh, P. K., Wang, H. J., Harth, C. M., Mühle, J., and Porter, L. W.: Renewed growth of atmospheric methane, *Geophys. Res. Lett.*, 35, L22805, doi:10.1029/2008GL036037, 2008.

25 Rödenbeck, C.: Estimating CO<sub>2</sub> sources and sinks from atmospheric mixing ratio measurements using a global inversion of atmospheric transport, *Tech. Rep. 6*, Max-Planck-Institut für Biogeochemie, Jena, available at: [http://www.bgc-jena.mpg.de/uploads/Publications/TechnicalReports/tech\\_report6.pdf](http://www.bgc-jena.mpg.de/uploads/Publications/TechnicalReports/tech_report6.pdf) (last access: 13 June 2014), Max-Planck-Institut für Biogeochemie, Jena, Germany, 2005.

30 Rödenbeck, C., Houweling, S., Gloor, M., and Heimann, M.: CO<sub>2</sub> flux history 1982–2001 inferred from atmospheric data using a global inversion of atmospheric transport, *Atmos. Chem. Phys.*, 3, 1919–1964, doi:10.5194/acp-3-1919-2003, 2003.

**Top-down estimates  
of European CH<sub>4</sub> and  
N<sub>2</sub>O emissions**

P. Bergamaschi et al.

Title Page

Abstract

Introduction

Conclusions

References

Tables

Figures



Back

Close

Full Screen / Esc

Printer-friendly Version

Interactive Discussion



Rödenbeck, C., Gerbig, C., Trusilova, K., and Heimann, M.: A two-step scheme for high-resolution regional atmospheric trace gas inversions based on independent models, *Atmos. Chem. Phys.*, 9, 5331–5342, doi:10.5194/acp-9-5331-2009, 2009.

Sanderson, M. G.: Biomass of termites and their emissions of methane and carbon dioxide: a global database, *Global Biogeochem. Cy.*, 10, 543–557, 1996.

Schmidt, M., Ramonet, M., Wastine, B., Delmotte, M., Galdemard, P., Kazan, V., Messenger, C., Royer, A., Valant, C., Xueref, I., and Ciais, P.: RAMCES: the French network of atmospheric greenhouse gas monitoring, in: 13th WMO/IAEA Meeting of Experts on Carbon Dioxide Concentration and Related Tracers Measurement Techniques, WMO report 168, ,Boulder, Colorado, USA, 19–22 September 2005, 165–174, 2006.

Shindell, D. T., Faluvegi, G., Bell, N., and Schmidt, G.: An emissions-based view of climate forcing by methane and tropospheric ozone, *Geophys. Res. Lett.*, 32, L04803, doi:10.1029/2004GL021900, 2005.

Stephens, B. B., Gurney, K. R., Tans, P. P., Sweeney, C., Peters, W., Bruhwiler, L., Ciais, P., Ramonet, M., Bousquet, P., Nakazawa, T., Aoki, S., Machida, T., Inoue, G., Vinnichenko, N., Lloyd, J., Jordan, A., Heimann, M., Shibistova, O., Langenfelds, R. L., Steele, L. P., Francey, R. J., and Denning, A. S.: Weak northern and strong tropical land carbon uptake from vertical profiles of atmospheric CO<sub>2</sub>, *Science*, 316, 1732–1735, 2007.

Thompson, R. L., Manning, A. C., Gloor, E., Schultz, U., Seifert, T., Hänsel, F., Jordan, A., and Heimann, M.: In-situ measurements of oxygen, carbon monoxide and greenhouse gases from Ochsenkopf tall tower in Germany, *Atmos. Meas. Tech.*, 2, 573–591, doi:10.5194/amt-2-573-2009, 2009.

Thompson, R. L., Bousquet, P., Chevallier, F., Rayner, P. J., and Ciais, P.: Impact of the atmospheric sink and vertical mixing on nitrous oxide fluxes estimated using inversion methods, *J. Geophys. Res.*, 116, D17307, doi:10.1029/2011JD015815, 2011.

Thompson, R. L., Ishijima, K., Saikawa, E., Corazza, M., Karstens, U., Patra, P. K., Bergamaschi, P., Chevallier, F., Dlugokencky, E., Prinn, R. G., Weiss, R. F., O'Doherty, S., Fraser, P. J., Steele, L. P., Krummel, P. B., Vermeulen, A., Tohjima, Y., Jordan, A., Haszpra, L., Steinbacher, M., Van der Laan, S., Aalto, T., Meinhardt, F., Popa, M. E., Moncrieff, J., and Bousquet, P.: TransCom N<sub>2</sub>O model inter-comparison, Part II: Atmospheric inversion estimates of N<sub>2</sub>O emissions, *Atmos. Chem. Phys. Discuss.*, 14, 5271–5321, doi:10.5194/acpd-14-5271-2014, 2014.



**Top-down estimates  
of European CH<sub>4</sub> and  
N<sub>2</sub>O emissions**

P. Bergamaschi et al.

Title Page

Abstract

Introduction

Conclusions

References

Tables

Figures



Back

Close

Full Screen / Esc

Printer-friendly Version

Interactive Discussion



Trusilova, K., Rödenbeck, C., Gerbig, C., and Heimann, M.: Technical Note: A new coupled system for global-to-regional downscaling of CO<sub>2</sub> concentration estimation, *Atmos. Chem. Phys.*, 10, 3205–3213, doi:10.5194/acp-10-3205-2010, 2010.

van der Werf, G. R., Randerson, J. T., Collatz, G. J., Giglio, L., Kasibhatla, P. S., Arellano Jr., A. F., Olsen, S. C., and Kasischke, E. S.: Continental-Scale Partitioning of Fire Emissions During the 1997 to 2001 El Nino/LaNina Period, *Science*, 303, 73–76, 2004.

Vermeulen, A. T., Schmidt, M., Manning, A., Moors, E., Moncrieff, J., Haszpra, L., Stefani, P., and Lindroth, A.: CHIOTTO, Final Report Rep. ECN-E-07-052, 118 pp., ECN, Petten, 2007.

Vermeulen, A. T., Hensen, A., Popa, M. E., van den Bulk, W. C. M., and Jongejan, P. A. C.: Greenhouse gas observations from Cabauw Tall Tower (1992–2010), *Atmos. Meas. Tech.*, 4, 617–644, doi:10.5194/amt-4-617-2011, 2011.

Wanninkhof, R.: Relationship between wind speed and gas exchange over the ocean, *J. Geophys. Res.*, 97, 7373–7382, 1992.

WMO: 16th WMO/IAEA Meeting on Carbon Dioxide, Other Greenhouse gases, and Related Measurement Techniques (Wellington, New Zealand, 25–28 October 2011), GAW Report No. 206 Rep., Geneva, Switzerland, 2012.

WMO: WMO greenhouse gas bulletin – The State of Greenhouse Gases in the Atmosphere Based on Global Observations through 2012 Rep., 4 pp., World Meteorological Organization, Geneva, 2013.











Title Page

Abstract

Introduction

Conclusions

References

Tables

Figures

◀

▶

◀

▶

Back

Close

Full Screen / Esc

Printer-friendly Version

Interactive Discussion



**Table 6.** CH<sub>4</sub> emissions from EDGARv4.1, EDGARv4.2, and UNFCCC for major CH<sub>4</sub> source categories. For the UNFCCC emissions, the reported relative uncertainties (2σ) per country and category and corresponding emission ranges are also compiled. Total uncertainties per country (or aggregated countries) are estimated from the reported uncertainties per category assuming no correlation between different UNFCCC categories (but correlated errors for sub-categories). “NWE” is the total of the north-western European countries Germany, France, UK, Ireland, and BENELUX. “NEE” is the total of the eastern European countries Hungary, Poland, Czech Republic (CZE) and Slovakia (SVK).

		Germany	France	UK + Ireland	BENELUX	Hungary	Poland	CZE + SVK	NWE	NEE	NWE + NEE	
<b>Solid Fuels (1B1)</b>												
emission (2005)	EDGARv4.1	Tg CH <sub>4</sub> yr <sup>-1</sup>	0.54	0.02	0.14	0.008	0.008	1.69	0.18	0.71	1.88	2.59
emission (2006–2007)	EDGARv4.2	Tg CH <sub>4</sub> yr <sup>-1</sup>	0.36	0.02	0.08	0.007	0.009	1.71	0.16	0.47	1.87	2.34
emission (2006–2007)	UNFCCC	Tg CH <sub>4</sub> yr <sup>-1</sup>	0.21	0.01	0.13	0.002	0.001	0.43	0.19	0.35	0.62	0.97
emission range	UNFCCC	Tg CH <sub>4</sub> yr <sup>-1</sup>	0.13–0.29	N/A <sup>2</sup>	0.11–0.14	0.001–0.002	0.022–0.64	0.16–0.21	0.25–0.45	0.38–0.85	0.64–1.30	
relative uncertainty	UNFCCC		37.4%	N/A <sup>2</sup>	13.0%	19.8%	10.4%	48.6%	13.2%	27.8%	37.9%	34.2%
<b>Oil and natural gas (1B2)</b>												
emission (2005)	EDGARv4.1	Tg CH <sub>4</sub> yr <sup>-1</sup>	0.37	1.44	0.66	0.26	0.08	0.15	0.07	2.73	0.30	3.03
emission (2006–2007)	EDGARv4.2	Tg CH <sub>4</sub> yr <sup>-1</sup>	0.27	1.49	0.61	0.28	0.08	0.15	0.08	2.64	0.31	2.95
emission (2006–2007)	UNFCCC	Tg CH <sub>4</sub> yr <sup>-1</sup>	0.28	0.05	0.27	0.06	0.10	0.21	0.07	0.66	0.38	1.03
emission range	UNFCCC	Tg CH <sub>4</sub> yr <sup>-1</sup>	0.25–0.32	0.04–0.06	0.22–0.32	0.04–0.07	0.05–0.15	0.20–0.22	0.04–0.09	0.55–0.76	0.29–0.46	0.84–1.23
relative uncertainty	UNFCCC		11.4%	18.0%	17.1%	30.2%	50.0%	5.3%	40.5%	15.9%	23.2%	18.5%
<b>Enteric fermentation (4A)</b>												
emission (2005)	EDGARv4.1	Tg CH <sub>4</sub> yr <sup>-1</sup>	1.06	1.39	1.50	0.50	0.09	0.58	0.22	4.45	0.89	5.34
emission (2006–2007)	EDGARv4.2	Tg CH <sub>4</sub> yr <sup>-1</sup>	1.04	1.37	1.48	0.50	0.09	0.58	0.21	4.40	0.88	5.27
emission (2006–2007)	UNFCCC	Tg CH <sub>4</sub> yr <sup>-1</sup>	0.99	1.36	1.20	0.48	0.08	0.44	0.14	4.04	0.66	4.70
emission range	UNFCCC	Tg CH <sub>4</sub> yr <sup>-1</sup>	0.66–1.32	1.15–1.58	0.98–1.42	0.39–0.58	0.07–0.09	0.29–0.59	0.11–0.17	3.17–4.91	0.47–0.85	3.64–5.76
relative uncertainty	UNFCCC		33.4%	15.8%	18.7%	20.3%	13.3%	34.4%	20.5%	21.5%	29.0%	22.6%
<b>Manure management (4B)</b>												
emission (2005)	EDGARv4.1	Tg CH <sub>4</sub> yr <sup>-1</sup>	0.35	0.36	0.25	0.25	0.03	0.15	0.04	1.21	0.21	1.42
emission (2006–2007)	EDGARv4.2	Tg CH <sub>4</sub> yr <sup>-1</sup>	0.35	0.35	0.25	0.25	0.03	0.14	0.03	1.20	0.20	1.40
emission (2006–2007)	UNFCCC	Tg CH <sub>4</sub> yr <sup>-1</sup>	0.26	0.48	0.24	0.19	0.07	0.16	0.03	1.17	0.26	1.43
emission range	UNFCCC	Tg CH <sub>4</sub> yr <sup>-1</sup>	0.18–0.34	0.33–0.62	0.18–0.29	0.04–0.35	0.06–0.09	0.09–0.23	0.02–0.04	0.73–1.61	0.16–0.36	0.89–1.97
relative uncertainty	UNFCCC		31.3%	30.4%	24.9%	80.4%	24.0%	44.6%	34.0%	37.8%	37.7%	37.8%
<b>Solid waste disposal on land (6A)</b>												
emission (2005)	EDGARv4.1	Tg CH <sub>4</sub> yr <sup>-1</sup>	0.60	0.08	1.12	0.35	0.10	0.44	0.08	2.14	0.63	2.76
emission (2006–2007)	EDGARv4.2	Tg CH <sub>4</sub> yr <sup>-1</sup>	0.51	0.34	1.07	0.28	0.11	0.33	0.15	2.20	0.58	2.78
emission (2006–2007)	UNFCCC	Tg CH <sub>4</sub> yr <sup>-1</sup>	0.76	0.48	0.84	0.25	0.15	0.39	0.20	2.32	0.73	3.06
emission range	UNFCCC	Tg CH <sub>4</sub> yr <sup>-1</sup>	0.38–1.14	0.00–0.96	0.44–1.24	0.16–0.34	0.10–0.19	0.04–0.73	0.06–0.35	0.97–3.67	0.20–1.27	1.17–4.94
relative uncertainty	UNFCCC		50.0%	102.0%	47.3%	36.2%	31.6%	89.2%	71.5%	58.2%	72.9%	61.7%
<b>Waste water (6B)</b>												
emission (2005)	EDGARv4.1	Tg CH <sub>4</sub> yr <sup>-1</sup>	0.17	0.19	0.12	0.13	0.03	0.09	0.09	0.60	0.21	0.82
emission (2006–2007)	EDGARv4.2	Tg CH <sub>4</sub> yr <sup>-1</sup>	0.17	0.19	0.12	0.13	0.03	0.10	0.08	0.60	0.21	0.82
emission (2006–2007)	UNFCCC	Tg CH <sub>4</sub> yr <sup>-1</sup>	0.01	0.06	0.09	0.01	0.02	0.05	0.04	0.17	0.12	0.28
emission range	UNFCCC	Tg CH <sub>4</sub> yr <sup>-1</sup>	0.00–0.01	0.00–0.12	0.05–0.13	0.01–0.02	0.02–0.03	0.01–0.09	0.02–0.07	0.05–0.28	0.04–0.19	0.09–0.47
relative uncertainty	UNFCCC		75.0%	104.4%	49.9%	45.4%	36.1%	88.1%	52.6%	68.8%	64.2%	66.9%
<b>total</b>												
total major categories	EDGARv4.1	Tg CH <sub>4</sub> yr <sup>-1</sup>	3.08	3.47	3.79	1.49	0.34	3.10	0.68	11.84	4.12	15.96
total major categories	EDGARv4.2	Tg CH <sub>4</sub> yr <sup>-1</sup>	2.70	3.76	3.60	1.45	0.34	3.01	0.71	11.50	4.06	15.57
total major categories	UNFCCC	Tg CH <sub>4</sub> yr <sup>-1</sup>	2.51	2.43	2.76	1.00	0.42	1.68	0.67	8.70	2.77	11.47
total all categories	UNFCCC	Tg CH <sub>4</sub> yr <sup>-1</sup>	2.65	2.56	2.83	1.07	0.43	1.83	0.71	9.11	2.97	12.08
total uncertainty	UNFCCC	Tg CH <sub>4</sub> yr <sup>-1</sup>	0.52	0.55	0.47	0.21	0.07	0.44	0.15	1.68	0.63	2.27
relative uncertainty	UNFCCC		20.6%	22.8%	16.8%	20.6%	17.0%	26.1%	22.9%	19.3%	22.8%	19.8%

<sup>1</sup> Recovery from coal mines not included in EDGARv4.1. <sup>2</sup> Uncertainty of CH<sub>4</sub> emissions from solid fuels in France not available.

## Top-down estimates of European CH<sub>4</sub> and N<sub>2</sub>O emissions

P. Bergamaschi et al.

Title Page

Abstract

Introduction

Conclusions

References

Tables

Figures



Back

Close

Full Screen / Esc

Printer-friendly Version

Interactive Discussion



**Table 7.** Bias of quasi-continuous N<sub>2</sub>O measurements. “CM-FM” denotes the annual average bias between quasi-continuous N<sub>2</sub>O measurements and NOAA discrete air samples (using measurements coinciding within 1 h, and the additional condition that the quasi-continuous measurements show low variability (max 0.3 ppb) within a 5 h time window; mean ± 1σ in units of ppb; *n*: number of coinciding measurements). The columns “TM5–4DVAR” and “LMDZ-4DVAR” give the bias corrections (vs. NOAA flask samples) calculated by the models for inversion S1 (for TM5-4DVAR calculated separately for 2006 and 2007, while LMDZ-4DVAR calculated the average bias over 2006–2007).

Station	CM-FM	TM5-4DVAR	CM-FM	TM5-4DVAR	LMDZ-4DVAR
	2006	2006	2007	2007	2006–2007
PAL	0.50 ± 0.33 ( <i>n</i> = 32)	0.46	0.31 ± 0.40 ( <i>n</i> = 40)	0.26	0.53
SIS		0.51		0.64	0.66
TT1		0.86		1.04	0.91
MHD	0.09 ± 0.29 ( <i>n</i> = 28)	−0.06	0.35 ± 0.53 ( <i>n</i> = 31)	0.06	0.13
BI5		0.27		0.21	0.19
CB3		0.31		0.59	0.70
OX3	1.07 ( <i>n</i> = 1)	1.29	0.73 ± 0.21 ( <i>n</i> = 3)	1.23	1.35
SIL		0.48		0.17	0.54
HU1	0.37 ± 0.83 ( <i>n</i> = 12)	0.38	0.58 ( <i>n</i> = 1)	0.39	0.26
JFJ		−0.41		−0.23	−0.26



## Top-down estimates of European CH<sub>4</sub> and N<sub>2</sub>O emissions

P. Bergamaschi et al.

**Table 8.** N<sub>2</sub>O emissions from EDGARv4.1, EDGARv4.2, and UNFCCC for major N<sub>2</sub>O source categories. For the UNFCCC emissions, the reported relative uncertainties (2σ) per country and category and corresponding emission ranges are also compiled. Total uncertainties per country (or aggregated countries) are estimated from the reported uncertainties per category assuming no correlation between different UNFCCC categories (but correlated errors for sub-categories). “NWE” is the total of the north-western European countries Germany, France, UK, Ireland, and BENELUX. “NEE” is the total of the eastern European countries Hungary, Poland, Czech Republic (CZE) and Slovakia (SVK).

			Germany	France	UK+Ireland	BENELUX	Hungary	Poland	CZE+SVK	NWE	NEE	NWE+NEE
<b>1A Fuel Combustion</b>												
emission (2005)	EDGARv4.1	Tg N <sub>2</sub> O yr <sup>-1</sup>	0.019	0.012	0.010	0.006	0.001	0.013	0.013	0.046	0.026	0.073
emission (2006–2007)	EDGARv4.2	Tg N <sub>2</sub> O yr <sup>-1</sup>	0.018	0.011	0.010	0.005	0.001	0.012	0.006	0.044	0.020	0.063
emission (2006–2007)	UNFCCC	Tg N <sub>2</sub> O yr <sup>-1</sup>	0.017	0.015	0.017	0.004	0.001	0.006	0.004	0.052	0.011	0.063
emission range	UNFCCC	Tg N <sub>2</sub> O yr <sup>-1</sup>	0.012–0.021	0.009–0.021	0.001–0.046	0.001–0.011	0.000–0.001	0.005–0.008	0.001–0.008	0.023–0.098	0.006–0.017	0.029–0.115
relative uncertainty	UNFCCC		26.2%	41.2%	95.3–176.7%	73.6–162.7%	71.2%	22.7%	76.3%	56.2–89.3%	47.1%	54.6–81.7%
<b>2B Chemical industry</b>												
emission (2005)	EDGARv4.1	Tg N <sub>2</sub> O yr <sup>-1</sup>	0.051	0.027	0.015	0.027	0.006	0.020	0.008	0.120	0.034	0.154
emission (2006–2007)	EDGARv4.2	Tg N <sub>2</sub> O yr <sup>-1</sup>	0.040	0.026	0.017	0.046	0.006	0.024	0.010	0.128	0.040	0.169
emission (2006–2007)	UNFCCC	Tg N <sub>2</sub> O yr <sup>-1</sup>	0.031	0.019	0.009	0.025	0.004	0.015	0.008	0.063	0.026	0.109
emission range	UNFCCC	Tg N <sub>2</sub> O yr <sup>-1</sup>	0.027–0.034	0.017–0.021	0.000–0.017	0.019–0.031	0.004–0.004	0.011–0.019	0.007–0.009	0.063–0.103	0.021–0.032	0.084–0.135
relative uncertainty	UNFCCC		11.1%	10.2%	100.0–100.4%	24.5%	2.2%	29.5%	13.9%	23.8%	21.1%	23.2%
<b>4B Manure management</b>												
emission (2005)	EDGARv4.1	Tg N <sub>2</sub> O yr <sup>-1</sup>	0.009	0.008	0.004	0.004	0.001	0.004	0.001	0.025	0.007	0.032
emission (2006–2007)	EDGARv4.2	Tg N <sub>2</sub> O yr <sup>-1</sup>	0.009	0.008	0.004	0.004	0.001	0.004	0.001	0.025	0.006	0.031
emission (2006–2007)	UNFCCC	Tg N <sub>2</sub> O yr <sup>-1</sup>	0.009	0.016	0.007	0.006	0.003	0.018	0.004	0.038	0.025	0.063
emission range	UNFCCC	Tg N <sub>2</sub> O yr <sup>-1</sup>	0.004–0.024	0.008–0.033	0.000–0.033	0.000–0.011	0.000–0.006	0.000–0.045	0.002–0.006	0.012–0.083	0.002–0.057	0.014–0.140
relative uncertainty	UNFCCC		60.8–69.1%	50.2%	100.0–349.6%	94.4–94.6%	100.0–100.3%	100.0–148.9%	54.7–54.9%	68.9–119.1%	93.2–129.2%	78.5–123.1%
<b>4D Agricultural soils</b>												
emission (2005)	EDGARv4.1	Tg N <sub>2</sub> O yr <sup>-1</sup>	0.086	0.098	0.077	0.025	0.012	0.052	0.013	0.285	0.077	0.363
emission (2006–2007)	EDGARv4.2	Tg N <sub>2</sub> O yr <sup>-1</sup>	0.084	0.096	0.075	0.025	0.012	0.050	0.013	0.280	0.075	0.355
emission (2006–2007)	UNFCCC	Tg N <sub>2</sub> O yr <sup>-1</sup>	0.129	0.155	0.111	0.035	0.017	0.056	0.022	0.431	0.095	0.525
emission range	UNFCCC	Tg N <sub>2</sub> O yr <sup>-1</sup>	0.036–0.337	0.000–0.565	0.002–0.509	0.005–0.091	0.000–0.064	0.022–0.091	0.007–0.037	0.043–1.502	0.029–0.193	0.072–1.695
relative uncertainty	UNFCCC		72.1–160.6%	100.0–264.9%	98.1–358.0%	87.1–158.3%	100.0–284.2%	61.5%	65.7–72.3%	90.1–248.9%	69.3–103.3%	86.3–222.6%
<b>6B Waste water</b>												
emission (2005)	EDGARv4.1	Tg N <sub>2</sub> O yr <sup>-1</sup>	0.007	0.006	0.005	0.002	0.001	0.003	0.001	0.020	0.005	0.025
emission (2006–2007)	EDGARv4.2	Tg N <sub>2</sub> O yr <sup>-1</sup>	0.007	0.006	0.006	0.002	0.001	0.003	0.001	0.020	0.005	0.025
emission (2006–2007)	UNFCCC	Tg N <sub>2</sub> O yr <sup>-1</sup>	0.008	0.003	0.004	0.002	0.001	0.004	0.001	0.017	0.005	0.023
emission range	UNFCCC	Tg N <sub>2</sub> O yr <sup>-1</sup>	0.007–0.009	0.000–0.006	0.000–0.020	0.001–0.004	0.000–0.010	0.002–0.005	0.000–0.001	0.008–0.039	0.002–0.017	0.010–0.056
relative uncertainty	UNFCCC		13.8%	100.0–104.4%	91.1–361.1%	70.8–75.3%	100.0–1000.0%	52.2%	54.4%	55.2–122.1%	61.0–218.9%	56.5–145.0%
<b>total</b>												
total major categories	EDGARv4.1	Tg N <sub>2</sub> O yr <sup>-1</sup>	0.172	0.150	0.112	0.064	0.021	0.092	0.036	0.497	0.149	0.646
total major categories	EDGARv4.2	Tg N <sub>2</sub> O yr <sup>-1</sup>	0.158	0.147	0.111	0.062	0.021	0.094	0.031	0.497	0.148	0.643
total major categories	UNFCCC	Tg N <sub>2</sub> O yr <sup>-1</sup>	0.194	0.207	0.147	0.072	0.025	0.099	0.038	0.621	0.163	0.784
total all categories	UNFCCC	Tg N <sub>2</sub> O yr <sup>-1</sup>	0.197	0.209	0.148	0.074	0.026	0.100	0.040	0.627	0.166	0.793
relative uncertainty	UNFCCC		48.3–107.3%	75.0–198.2%	75.1–271.3%	43.9–78.1%	67.5–192.7%	39.8–44.6%	38.6–42.2%	62.9–173.0%	43.0–63.8%	58.5–149.8%

[Title Page](#)
[Abstract](#)
[Introduction](#)
[Conclusions](#)
[References](#)
[Tables](#)
[Figures](#)
[Back](#)
[Close](#)
[Full Screen / Esc](#)
[Printer-friendly Version](#)
[Interactive Discussion](#)


Top-down estimates of European CH<sub>4</sub> and N<sub>2</sub>O emissions

P. Bergamaschi et al.

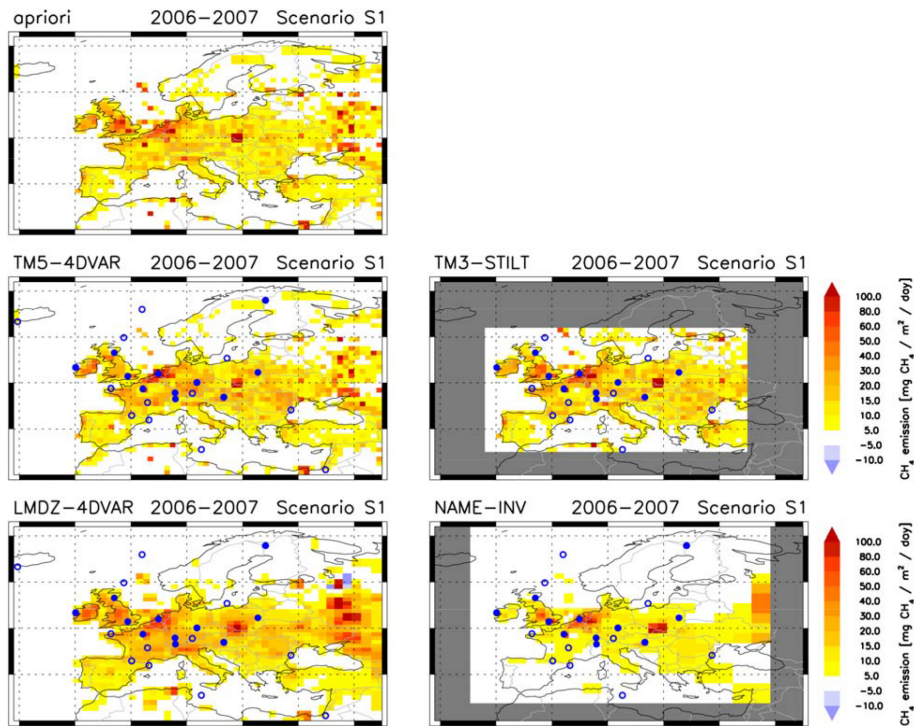


**Figure 1.** European CH<sub>4</sub> emissions (average 2006–2007, inversion S1–CH<sub>4</sub>). Filled circles are measurement stations with quasi-continuous measurements, and open circles discrete air sampling sites.

Top-down estimates  
of European  $\text{CH}_4$  and  
 $\text{N}_2\text{O}$  emissions

P. Bergamaschi et al.

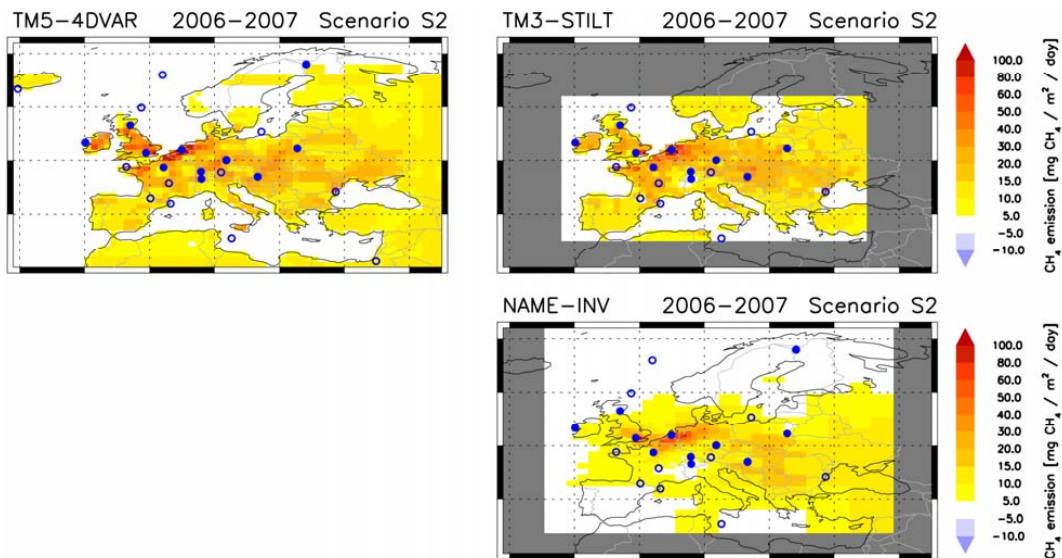


**Figure 2.** European  $\text{CH}_4$  emissions (average 2006–2007, inversion S2- $\text{CH}_4$ ). Filled circles are measurement stations with quasi-continuous measurements, and open circles discrete air sampling sites.

[Title Page](#)[Abstract](#)[Introduction](#)[Conclusions](#)[References](#)[Tables](#)[Figures](#)[◀](#)[▶](#)[◀](#)[▶](#)[Back](#)[Close](#)[Full Screen / Esc](#)[Printer-friendly Version](#)[Interactive Discussion](#)

## Top-down estimates of European CH<sub>4</sub> and N<sub>2</sub>O emissions

P. Bergamaschi et al.

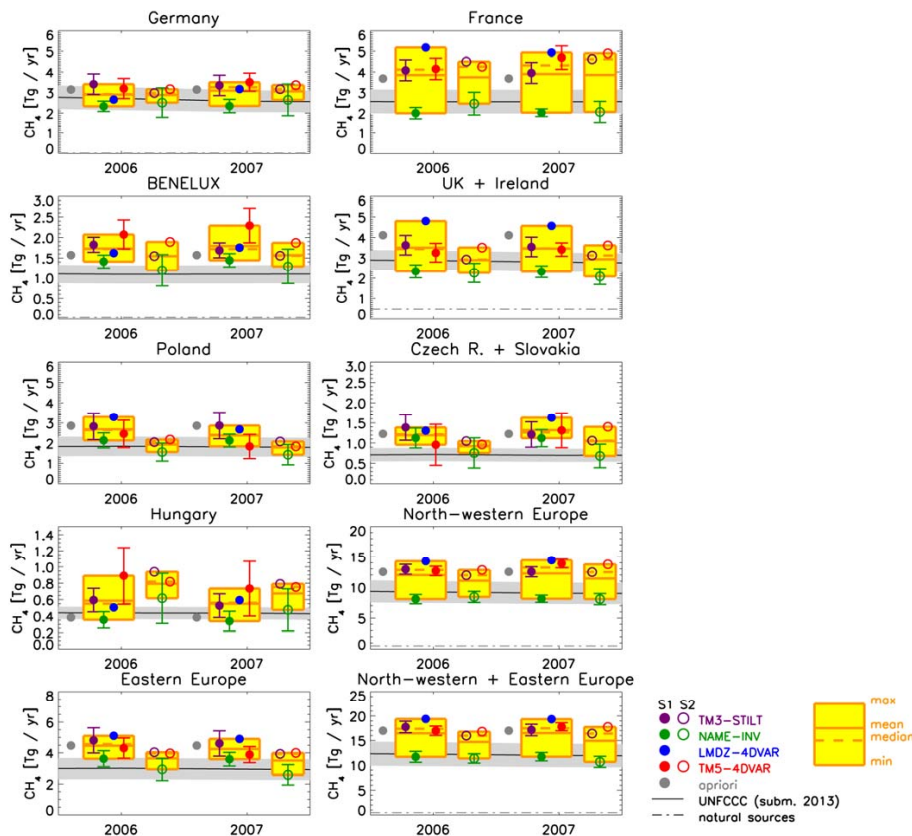


**Figure 3.** European CH<sub>4</sub> emissions by country and aggregated region. For each year, the left yellow box shows the results for inversion S1–CH<sub>4</sub>, and the yellow right box for S2–CH<sub>4</sub>. The grey-shaded area is the range of UNFCCC CH<sub>4</sub> emissions (based on reported uncertainties, as compiled in Table 6).

## Top-down estimates of European CH<sub>4</sub> and N<sub>2</sub>O emissions

P. Bergamaschi et al.

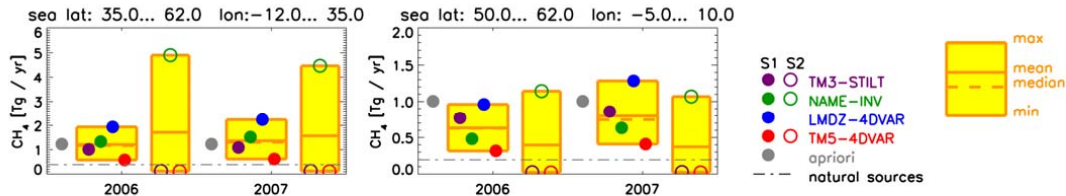


**Figure 4.** CH<sub>4</sub> emissions over European seas. Left: total CH<sub>4</sub> emissions between 35° and 62° N, and 12° W and 35° E, representing the largest common domain of all models; right: total CH<sub>4</sub> emissions over the North Sea.

[Title Page](#)
[Abstract](#)
[Introduction](#)
[Conclusions](#)
[References](#)
[Tables](#)
[Figures](#)
[Back](#)
[Close](#)
[Full Screen / Esc](#)
[Printer-friendly Version](#)
[Interactive Discussion](#)


## Top-down estimates of European CH<sub>4</sub> and N<sub>2</sub>O emissions

P. Bergamaschi et al.

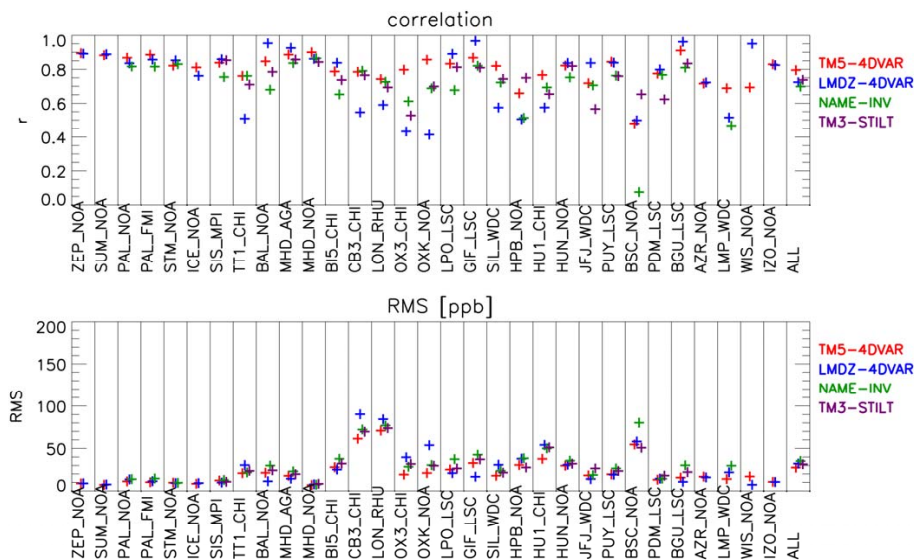


**Figure 5.** Comparison of modeled and observed CH<sub>4</sub> at stations: correlation coefficients (top) and root mean square (RMS) differences (bottom) for inversion S1–CH<sub>4</sub>. “All” denotes the mean correlation coefficient and RMS difference, averaged over those stations, for which results were available from all models.

Title Page

Abstract

Introduction

Conclusions

References

Tables

Figures



Back

Close

Full Screen / Esc

Printer-friendly Version

Interactive Discussion



## Top-down estimates of European CH<sub>4</sub> and N<sub>2</sub>O emissions

P. Bergamaschi et al.

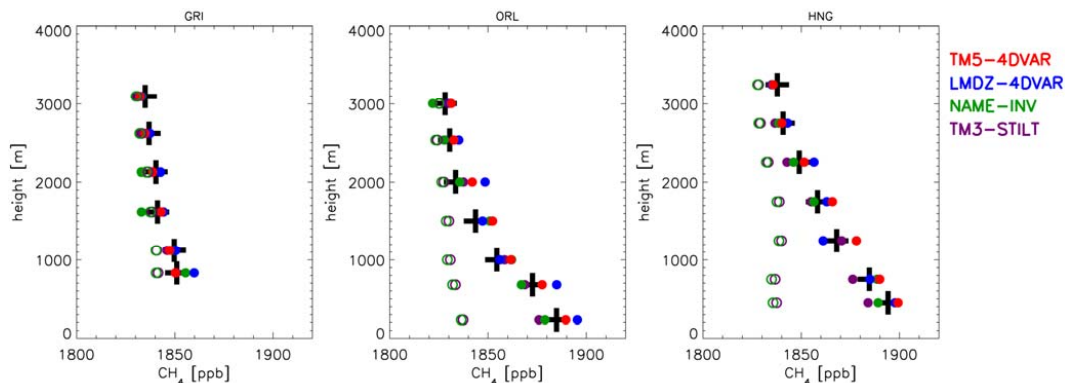


**Figure 6.** GEOMON aircraft profile measurements of CH<sub>4</sub> at Griffin (Scotland), Orleans (France), and Hegyhatsal (Hungary) used for validation of atmospheric models. The figure shows the average over all available measurements (black crosses) during 2006–2007 and average of corresponding model simulations (filled colored symbols; for NAME-INV only a subset of aircraft profiles had been provided). The open colored circles show the calculated background mixing ratios applied for the limited domain model NAME-INV and STILT, based on the method of Rödenbeck et al. (2009).

Title Page

Abstract

Introduction

Conclusions

References

Tables

Figures



Back

Close

Full Screen / Esc

Printer-friendly Version

Interactive Discussion



## Top-down estimates of European CH<sub>4</sub> and N<sub>2</sub>O emissions

P. Bergamaschi et al.

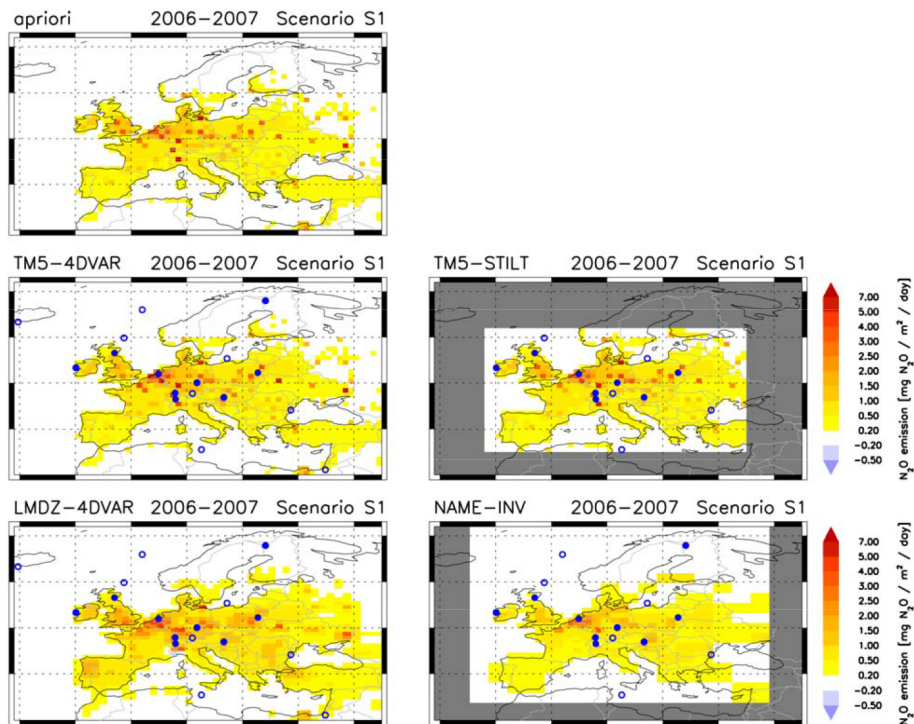


**Figure 7.** European N<sub>2</sub>O emissions (average 2006–2007, inversion S1–N<sub>2</sub>O). Filled circles are measurement stations with quasi-continuous measurements, and open circles discrete air sampling sites.

[Title Page](#)
[Abstract](#)
[Introduction](#)
[Conclusions](#)
[References](#)
[Tables](#)
[Figures](#)
[Back](#)
[Close](#)
[Full Screen / Esc](#)
[Printer-friendly Version](#)
[Interactive Discussion](#)



## Top-down estimates of European CH<sub>4</sub> and N<sub>2</sub>O emissions

P. Bergamaschi et al.

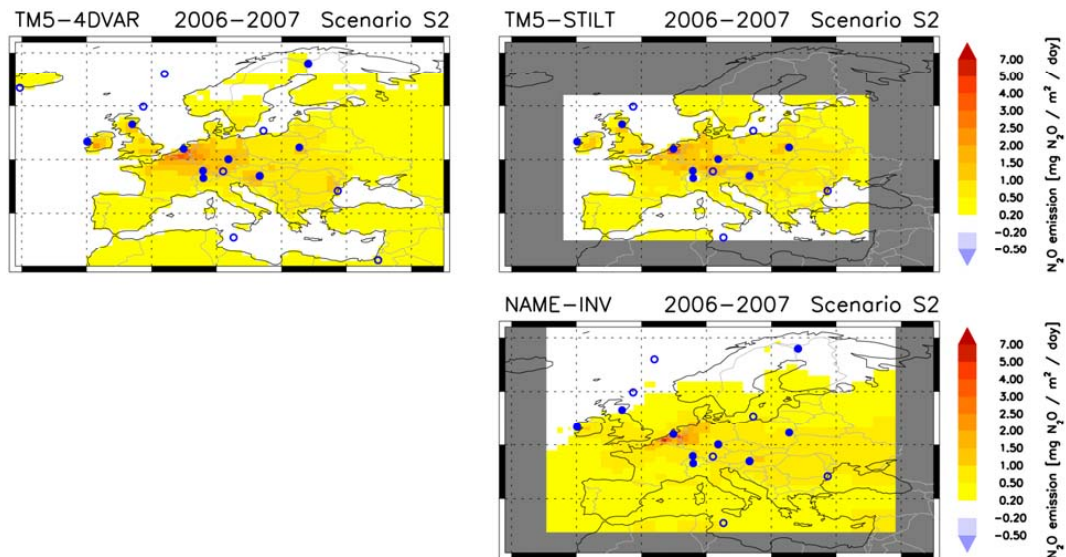


**Figure 8.** European N<sub>2</sub>O emissions (average 2006–2007, inversion S2–N<sub>2</sub>O). Filled circles are measurement stations with quasi-continuous measurements, and open circles discrete air sampling sites.

Title Page

Abstract

Introduction

Conclusions

References

Tables

Figures

◀

▶

◀

▶

Back

Close

Full Screen / Esc

Printer-friendly Version

Interactive Discussion



Top-down estimates of European CH<sub>4</sub> and N<sub>2</sub>O emissions

P. Bergamaschi et al.

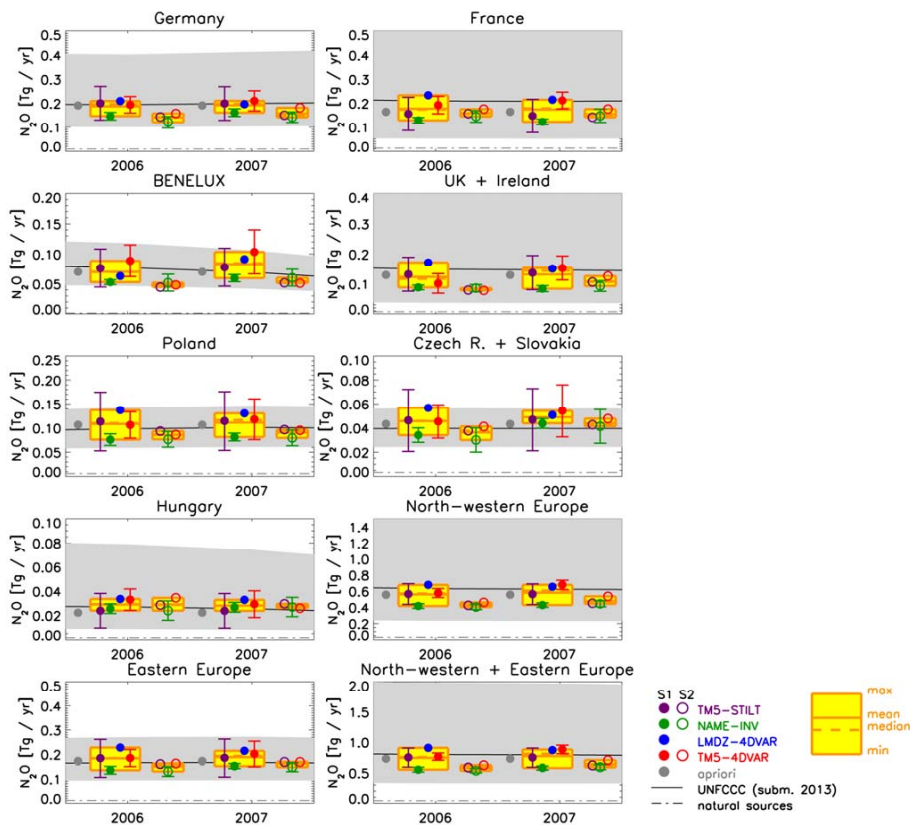


**Figure 9.** European N<sub>2</sub>O emissions by country and aggregated region. For each year, the left yellow box shows the results for inversion S1–N<sub>2</sub>O, and the yellow right box for S2–N<sub>2</sub>O. The grey-shaded area is the range of UNFCCC N<sub>2</sub>O emissions (based on reported uncertainties, as compiled in Table 8; note that for some countries the UNFCCC range exceeds the scale of figures).

Title Page

Abstract

Introduction

Conclusions

References

Tables

Figures

◀

▶

◀

▶

Back

Close

Full Screen / Esc

Printer-friendly Version

Interactive Discussion





## Top-down estimates of European CH<sub>4</sub> and N<sub>2</sub>O emissions

P. Bergamaschi et al.

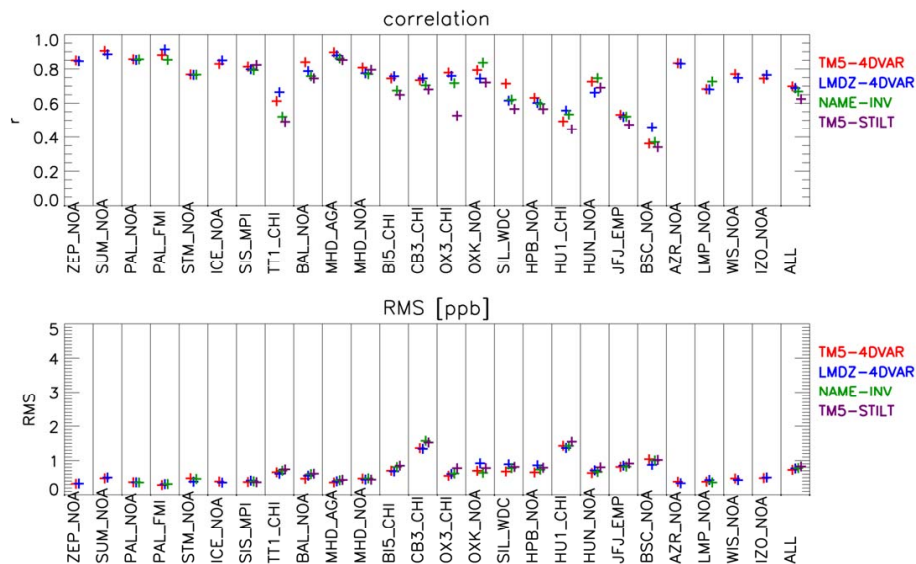


**Figure 11.** Comparison of modeled and observed N<sub>2</sub>O at stations: correlation coefficients (top) and root mean square (RMS) differences (bottom) for inversion S1–N<sub>2</sub>O (after bias correction of observations). “All” denotes the mean correlation coefficient and RMS difference, averaged over those stations, for which results were available from all models.

Title Page

Abstract

Introduction

Conclusions

References

Tables

Figures



Back

Close

Full Screen / Esc

Printer-friendly Version

Interactive Discussion

